Parameterization method for unstable manifolds of delay differential equations

Chris Groothedde * [1] and J.D. Mireles James †[2]

[1]Vrije Universiteit Amsterdam, Department of Mathematics
[2]Florida Atlantic University, Department of Mathematical Sciences

October 14, 2016

Abstract

This work concerns efficient numerical methods for computing high order Taylor and Fourier-Taylor approximations of unstable manifolds attached to equilibrium and periodic solutions of delay differential equations. In our approach we first reformulate the delay differential equation as an ordinary differential equation on an appropriate Banach space. Then we extend the Parameterization Method for ordinary differential equations so that we can define operator equations whose solutions are charts or covering maps for the desired invariant manifolds of the delay system. Finally we develop formal series solutions of the operator equations. Order-by-order calculations lead to linear recurrence equations for the coefficients of the formal series solutions. These recurrence equations are solved numerically to any desired degree.

The method lends itself to a-posteriori error analysis, and recovers the dynamics on the manifold in addition to the embedding. Moreover, the manifold is not required to be a graph, hence the method is able to follow folds in the embedding. In order to demonstrate the utility of our approach we numerically implement the method for some 1,2,3 and 4 dimensional unstable manifolds in problems with constant, and (briefly) state dependent delays.

Keywords: delay differential equations, constant and state dependent delays, local unstable manifolds, equilibrium solutions, periodic solutions, parametrization method, Wright's equation.

AMS Subject Classifications: 37D05, 37D10, 37L10, 37M99, 65P99, 34K19, 34K28

1 Introduction

Numerical methods for computing stable/unstable manifolds occupy a central position in the field of computational dynamics. Many of these methods fall into one of two varieties: techniques for computing a local representation of the manifold in terms of its jets, and continuation methods for extending a local representation as far as possible via numerical

*Email: `c.m.groothedde@vu.nl`

†J.M.J partially supported by NSF grant DMS - 1318172 Email: `jmirelesjames@fau.edu`

integration. The present work is a new offering of the first variety, and develops numerical methods for high order approximations of local unstable manifolds of delay differential equations (DDEs). Differential equations with delays model systems "with memory", i.e. systems whose next state depends not only on their current state but also on some portion of the past history. Dependance on past history makes the state space of a DDE an infinite dimensional function space, complicating both theoretical and numerical work.

Our approach is based on a general functional analytic framework for studying invariant manifolds known as *the parameterization method*, developed by a number of authors over the last years [4, 5, 6, 32, 30, 31, 29]. Loosely speaking, the parameterization method leads to an operator equation whose solutions parameterize the desired invariant manifold. The operator equation is solved via a formal series/power matching argument, which leads to linear equations for the jets of the manifold. Numerically solving finitely many of these linear equations provides a polynomial approximation of the manifold of whatever degree we wish.

The parameterization method has several important features. First, the operator equation describes an infinitesimal conjugacy relation between the nonlinear dynamics on the unstable manifold and the dynamics in the unstable subspace of the linearized system. Due to this fact, the method recovers the dynamics on the manifold in addition to its embedding. Second, the parameterization is not required to be the graph of a function, hence can follow folds in the embedding as we will see in the applications below. Finally, the fact that the parameterization solves an operator equation also leads to a convenient notion of a-posteriori error or defect, which is used in applications to measure the quality of the final polynomial approximation.

Even though the original references [4, 5, 6] framed the parameterization method in the general setting of infinite dimensional Banach spaces, the results there require invertibility of certain linear operators, and do not apply directly to the unbounded linear operators which appear in the context of DDEs. Many subsequent works on the parameterization method provide extensions of the parameterization method to problems involving unbounded operators. For example the works of [55, 60, 21] develop/discuss computational methods for studying unstable manifolds attached to equilibrium and periodic orbits for some infinite dimensional systems. However the techniques developed in these references focus on parabolic PDEs/compact maps, hence still do not apply directly to the DDE setting. Many other extensions to problems involving unbounded operators (including some recent work on DDEs) focus on quasi-periodic solutions and KAM techniques. See Section 2 for more discussion of this point.

Since we are interested in parameterizing unstable manifolds we begin by recasting the DDE as an ODE on an appropriate Banach space, and then work out the implications of the parameterization method "from scratch" for this ODE. The reformulation of a DDE as an ODE is completely classical, however since it is critical to our entire approach we provide a detailed review in Section 2. The advantage of carefully developing the parameterization method in the classical context of *retarded functional differential equations* is that the correct form of the series expansion for the unstable manifold appears quite naturally as the results of a certain formal computation.

We develop the desired machinery for equilibrium as well as periodic solutions of DDEs. We illustrate the utility of the proposed method by working a number of example problems. More precisely we compute some high order Taylor and Fourier-Taylor approximations of one, two, three, and four dimensional unstable manifolds for three different example systems: two with constant and one with a state dependent delay.

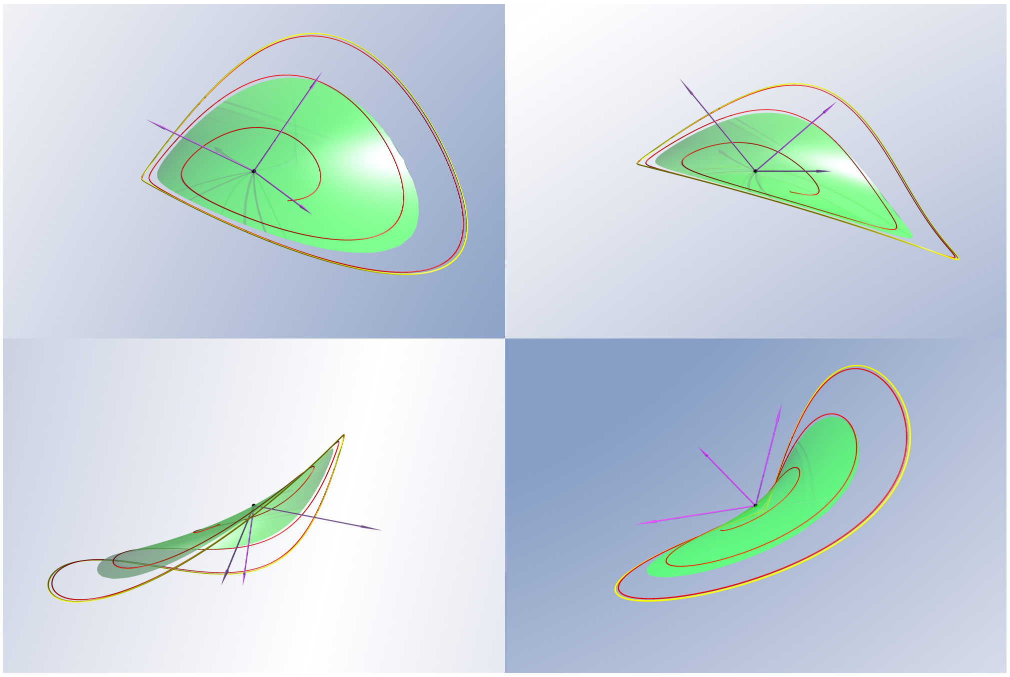

Figure 1: Parameterization of a 2D local unstable manifold attached to the origin for Wright's equation with $\alpha = 2.2$. The system has an attracting periodic orbit (yellow). We integrate an orbit (red) on the local unstable manifold until it converges to the periodic orbit. We compute the parameterization to Taylor order $K = 130$ by solving the recurrence Equation (4). The coordinates used in the figure are discussed in Section 2.1.3.

1.1 Sketch of the method

Before we undertake the systematic formulation of the parameterization method for unstable manifolds of delay differential equations (which requires both a detailed review of some basic dynamical systems theory for DDEs, as well as some general discussion of the parameterization method for unstable manifolds of equilibria and periodic orbits) we would like to motivate the more technical discussion to come with brief and informal account of our method, along with some illustrative example computations.

Consider the delay differential equation

$$u'(t) = f(u(t), u(t-1)), \tag{1}$$

with $f\colon \mathbb{R}^2 \to \mathbb{R}$ a smooth (say analytic) function, and suppose that $u_0(t) \equiv c$ is an equilibrium solution, i.e. assume that

$$f(c, c) = 0.$$

Moreover, suppose that u_0 is an unstable equilibrium with exactly $m \in \mathbb{N}$ distinct unstable eigenvalues. More precisely this assumes that there are exactly m complex numbers $\lambda_1, \ldots, \lambda_m \in \mathbb{C}$ with $\mathrm{real}(\lambda_j) > 0$ for $1 \le j \le m$, solving the transcendental *characteristic equation*

$$\partial_1 f(c, c) + \partial_2 f(c, c) e^{-\lambda} = \lambda.$$

Associated eigenfunctions are given by

$$\xi_j(t) = s_j e^{\lambda_j t},$$

for $1 \leq j \leq m$, where $s_j \in \mathbb{R}$ are arbitrary scalings. (This standard material is reviewed in Section 2).

Loosely speaking, the results of Section 4.1 show the following: suppose that $P\colon \mathbb{R}^m \to C^k((-\infty, 0], \mathbb{R})$ satisfies the *invariance equation*

$$\sum_{j=1}^{m} \lambda_j \sigma_j \frac{\partial}{\partial \sigma_j} P(\sigma_1, \dots, \sigma_m, t) = f(P(\sigma_1, \dots, \sigma_m, t), P(\sigma_1, \dots, \sigma_m, t-1)), \tag{2}$$

for $|\sigma_j| < 1$, $1 \leq j \leq m$, and $t \leq 0$, subject to the constraints

$$P(0, \dots, 0, t) = c,$$

$$\frac{\partial}{\partial \sigma_j} P(0, \dots, 0, t) = \xi_j(t),$$

for $1 \leq j \leq m$. Then P parameterizes an m-dimensional local unstable manifold of u_0.

In order to solve Equation (2), we make the power series *ansatz*

$$P(\sigma_1, \dots, \sigma_m, t) = \sum_{\alpha_1=0}^{\infty} \dots \sum_{\alpha_j=0}^{\infty} p_{\alpha_1 \dots \alpha_j} e^{(\alpha_1 \lambda_1 + \dots + \alpha_m \lambda_m)t} \sigma_1^{\alpha_1} \dots \sigma_m^{\alpha_m}, \tag{3}$$

with $\{p_{\alpha_1 \dots \alpha_m}\}_{\alpha_1, \dots, \alpha_m \in \mathbb{N}}$ unknown. The first order constraints imply that

$$p_{0\dots 0} = c, \qquad p_{10\dots 0} = s_1, \qquad \dots \qquad p_{0\dots 01} = s_m,$$

i.e. that the zeroth order coefficient is the constant solution and the first order coefficients are the eigenvector scalings. Plugging the right hand side of Equation (3) into Equation (2), expanding the composition as a power series, and matching like powers of $\sigma_1, \dots, \sigma_m$, leads to equations for the unknown coefficient $p_{\alpha_1 \dots \alpha_m}$ in terms of lower order coefficients.

Consider for example Wright's equation, where $f\colon \mathbb{R}^2 \to \mathbb{R}$ is given by

$$f(x, y) = -\alpha y(1 + x), \qquad \alpha \in \mathbb{R}.$$

The constant function $u_0(t) \equiv 0$ is an equilibrium solution, and when $\pi/2 < \alpha < 5\pi/2$ the origin has exactly two unstable (complex conjugate) eigenvalues. Then $p_{00} = 0$ and $p_{01} = p_{10}$ are arbitrary. The power matching scheme described above leads to the recurrence relations

$$p_{mn} = -\frac{\alpha}{(m\lambda_1 + n\lambda_2) + \alpha e^{-(m\lambda_1 + n\lambda_2)}} \sum_{j=0}^{m} \sum_{k=0}^{n} c_{jk}^{mn} p_{m-j\, n-k} p_{jk} e^{-(j\lambda_1 + k\lambda_2)}, \tag{4}$$

for $m, n \in \mathbb{N}$ with $m + n \geq 2$. Here

$$c_{jk}^{mn} := \begin{cases} 0 & \text{if } j = 0 \text{ and } k = 0 \\ 0 & \text{if } j = m \text{ and } k = n \\ 1 & \text{otherwise} \end{cases},$$

appears in the right hand side because the p_{mn} term is extracted from the Cauchy product summation, i.e. the right hand side of Equation (4) depends only on terms or order less

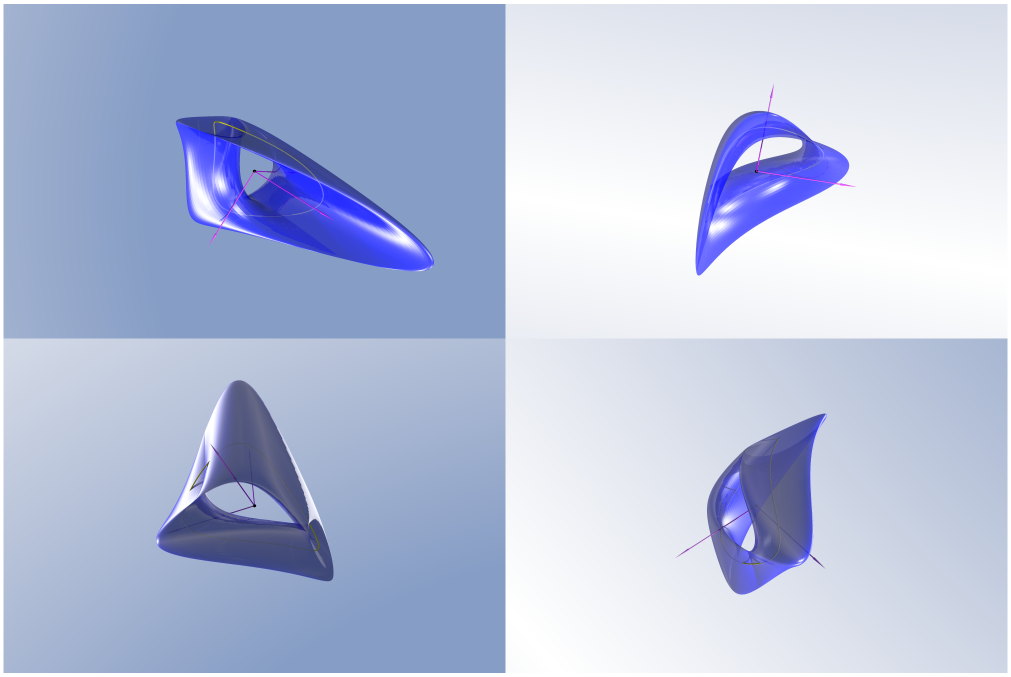

Figure 2: Boundary torus of a parameterized local unstable manifold attached to a periodic orbit for Wright's equation with $\alpha = 9$. We compute to Taylor order $K = 42$ and Fourier order $M = 22$. The surface plotted in the frames is obtained by evaluating and plotting the image of the resulting Fourier-Taylor polynomial and exploits no numerical integration procedures. The torus is embedded in an infinite dimensional phase space so has no inside and outside. The coordinates used in the figure are discussed in Section 2.1.3.

than $m + n$. (Note that $c_{jk}^{mn} := 1 - \delta_{jk}^{mn}$ in terms of the standard Kronecker delta). Now, for any $K \in \mathbb{N}$ we begin with the cases $m + n = 2$ and recursively compute p_{mn} for all $2 \leq m + n \leq K$ using the formula of Equation (4). The result is a truncated series (i.e. polynomial) approximation of P. Some results are illustrated in Figure 1. Numerical considerations such as the domain of P, and the decay rates of the coefficients are considered in detail in Section 5.

Remark 1.1 (Goals of the present work)**.** The ansatz of Equation (3) (note the exponential weight functions) as well as the invariance Equation (2) in the discussion above are drawn out of thin air. In fact the entire discussion above is somewhat informal. To give dynamical meaning to objects like the local unstable manifold and to the invariance Equation (2), it is necessary to first reformulate the DDE as an ODE on a Banach space. The results in Sections 3 and 4 justify and generalize the above discussion.

Remark 1.2 (Parameterized local unstable manifold attached to a periodic orbit)**.** Another goal of the present work is to develop a parameterization method for unstable manifolds attached to periodic solutions of DDEs. In the periodic case the appropriate operator equation is a generalization of Equation (2), and the generalized operator equation is solved using a power series ansatz whose coefficients are given by periodic functions rather than scalars. The appropriate invariance Equation (35) is developed in Section 4.2. In the periodic case the power matching argument gives that the recursion equations describing the jets are linear delay differential equations with periodic data. Such equations are efficiently solved in Fourier space.

Figure 2 illustrates the results of a computation using our method for an unstable periodic orbit for Wright's equation. The periodic orbit has exactly two (complex conjugate) unstable Floquet exponents, so that the local unstable manifold is a three dimensional tube. The figure illustrates a boundary torus of this tube. The image is generated by evaluating the Fourier-Taylor polynomial computed as indicated in the previous paragraph. Numerical considerations are discussed in detail in Section 5.

Remark 1.3 (Stable versus unstable manifolds)**.** The appearance of certain denominators in the recursive formula for p_{mn} given by Equation (4) lead to some *non-resonance* conditions which must hold between the unstable eigenvalues. These non-resonance conditions do not involve stable or center eigenvalues. As we will see again below, such non-resonance conditions are an unavoidable feature of the parameterization method. Indeed they are the price to be paid for the fact that the method recovers the dynamics on the manifold, in addition to the embedding.

The DDEs considered in the present work all have have the following property: that the linearized operators at the equilibrium/periodic solutions generate eventually compact semi-groups. Due to this fact, we will always have only a finite number of unstable eigenvalues each with only finite multiplicity. This compactness is exactly why we can apply the parameterization method to study unstable manifolds of DDEs. Stable manifolds (which will have finite co-dimension) must be studied by other methods. However this situation is no different form that encountered when studying dynamical systems generated by compact integral operators or parabolic PDEs, where the parameterization method has proven quite valuable. See for example [55, 15, 60]. We will return to the topic of stable manifolds in a future work.

1.2 Related Work

Three works closely related to the present study are the recent papers [52] and [34, 35]. The authors use functional analytic techniques based on the parameterization method to prove the existence of quasi-periodic solutions of differential equations with constant and state dependent delays. The analysis employed in these works is perturbative, yet by analogy with the finite dimensional case (see for example [32, 30, 31, 7, 14]) it is reasonable to suppose that the arguments of [52, 34, 35] lead to efficient numerical methods for computing quasi-periodic solutions of delay differential equations. Indeed, this is an excellent topic for future study.

The success of [52, 34, 35] suggests also that the related work of [4, 5, 6] on stable/unstable manifolds attached to equilibria of differential equations should be adapted to DDEs. A number of authors have developed numerical methods for studying stable/unstable manifolds based on the works of [4, 5, 6], see for example [56, 3, 61, 53, 11, 55, 60]. Indeed some of these works treat periodic orbits of ODEs and also unstable manifolds for PDEs. All of these developments taken together suggest novel methods for computing invariant manifolds attached to equilibrium and periodic solutions of delay differential equations, and motivate the present study.

The present work is also related to several other studies which develop numerical methods for stable/unstable manifolds attached to invariant objects of DDEs. Theoretical aspects of discretization of unstable manifolds for delay equations are studied in [19]. The work of [63] develops numerical methods for computing two dimensional unstable manifolds attached to equilibrium solutions of delay differential equations with constant delays. We also mention the work of [47, 24] on numerical computation of unstable manifolds of periodic orbits with a single unstable Floquet exponent. The work of [9] develops formal series expansions of center manifolds for delay differential equations implementing normal form techniques in the Maple programing language. More recently the work of [8] studies numerically a center manifold normal form for a Hopf-Hopf bifurcation in a system with two state dependent delays. The authors compute and continue families of invariant tori including resonant invariant tori.

In the sequel we are also interested in accurate Fourier representation of periodic orbits for delay differential equations. Our approach is based on the work of [48, 43, 44]. The methods of the works just cited are used also to give mathematically rigorous computer assisted proofs of the existence of periodic orbits for delay equations. The interested reader can consult also the lecture notes [49]. In addition we discuss a modification of these methods which allows us to parameterize the unstable vector bundles of the periodic orbit, leading again to accurate Fourier representations.

The work of [17] uses set-oriented methods to find cubical enclosures of relative attractors for delay equations. We also mention the work of [68] on rigorous numerical integration of DDEs, and computer assisted proof of periodic orbits. The reader interested in the dynamical systems approach to numerical computations for delay equations can consult also the studies of [20, 38, 62, 1, 64, 18]. Some numerical studies of physical applications from a dynamical systems perspective are found in [66, 36, 38, 16]. The discussion of the literature in this section is of course far from comprehensive, and the interested reader will find many other works of interest by consulting the references in the papers cited above.

Remark 1.4 (Local manifold computation versus manifold extension/continuation)**.** The works [63, 47, 24] just cited develop methods for numerical approximation of global stable/unstable manifolds given a good local approximation of the manifold. Put simply these methods extend the local manifolds by combining numerical integration techniques with adaptive continuation/collocation methods. Such computations are delicate as the nonlinearities act on different regions of the manifold in very different ways, causing some parts of the manifold to "move" or "grow" very rapidly while others move very slowly. An excellent survey describing a number of extension/globalization methods for stable/unstable manifolds attached to equilibria of ODEs is [46]. See also the references discussed therein.

The present work, on the other hand, develops methods for high order approximation of local invariant manifolds, but ignores the extension/globalization of these objects. We do wish to emphasize however that the two approaches are complementary rather than competitive, and this suggests interesting possible directions for future research. More precisely: while extension/globalization computations are typically seeded with the linear approximation of the invariant manifold by its unstable eigenvectors, nothing prevents the seeding these algorithms with a high order local approximation as developed in the present work. Indeed the two studies [74, 23] show that combining the parameterization method with adaptive extension/globalization methods produces excellent results, at least in the case of one and two dimensional manifolds attached to fixed points of diffeomorphisms. Developing similar methods for ODEs and DDEs is an interesting topic for future study.

2 Background

This sections recalls the dynamical systems approach to delay differential equations, i.e. we describe how such problems lead to ODEs on a function space. We consider a somewhat larger class of problems than introduced in Section 1.1. This material is classical, but we

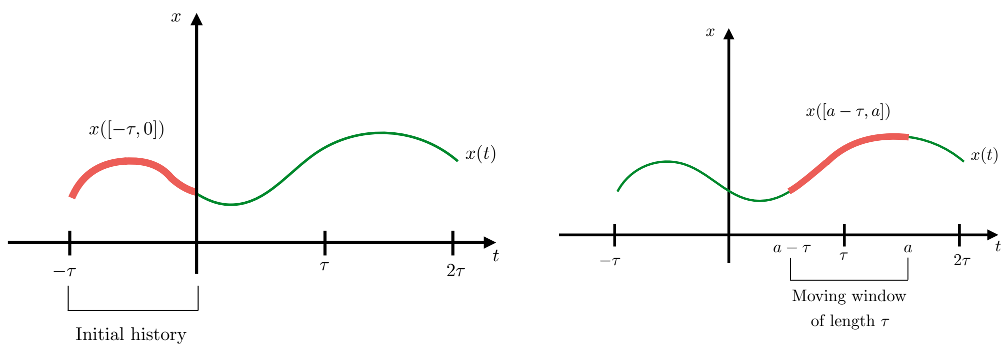

Figure 3: Left frame: solution of a delay equation with initial history segment colored in red. Right frame: solution of same delay equation with the evolution of the initial segment by time $t = a$ colored red.

include it to give a self contained presentation. For more complete exposition of this material we refer to the works of [26, 27, 33, 71]. We also describe the embedding coordinates used to plot the orbits and manifolds throughout the present work. The reader familiar with these notions may want to skim or skip Section 2, and refer back to it only as needed.

2.1 Functional differential equations: delay equations as ODEs on a Banach space

An autonomous, scalar, delay differential equation, with one constant delay of $\tau > 0$ is an equation of the form

$$\frac{d}{dt}x(t) = f(x(t), x(t-\tau)), \tag{5}$$

where $f\colon \mathbb{R}^2 \to \mathbb{R}$ is a smooth function. Note that the solution on the interval $[0,\tau]$ depends on the the function values of $x(t)$ on $[-\tau, 0]$. For example $x'(0) = f(x(0), x(\tau))$ and more generally $x'(\epsilon) = f(x(\epsilon), x(\epsilon-\tau))$ for $\epsilon \in [0,\tau]$. Then the initial history segment $x|_{[-\tau,0]}$ must be specified in order to determine the forward solution. The situation is illustrated in Figure 5, and captures the major difference between ordinary and delay differential equations.

Similarly, the equation is said to have n constant delays $0 < \tau_1 < \ldots < \tau_n$ if it is of the form

$$\frac{d}{dt}x(t) = f(x(t), x(t-\tau_1), \ldots, x(t-\tau_n)), \tag{6}$$

for a smooth function $f\colon \mathbb{R}^{n+1} \to \mathbb{R}$.

More generally an autonomous delay differential equation (with maximum delay τ) is given by the functional differential equation

$$u'(t) = F(u_t), \tag{7}$$

where $F : C[-\tau, 0] \to \mathbb{C}$ and where for each $t \in [\tau, \infty)$ we define $u_t : [-\tau, 0] \to \mathbb{C}$ by $u_t(s) = u(t+s)$. For each t the function $u_t \in C[-\tau, 0]$ represents the "history" of the function u at time t that is relevant with respect to the delay τ. Since the derivative in each t can depend on all values in $[t-\tau, t]$, an initial condition for (7) must be a function on $[-\tau, 0]$.

Using this formalism, we can distinguish different types of DDEs, namely *constant-delay differential equations* and *state-dependent delay differential equations.*

Definition 2.1 (DDEs with constant delay)**.** We say that the functional differential equation in (7) has a constant delay if there exist $\tau_1, \ldots, \tau_n \in [-\tau, 0]$ such that $F : C[-\tau, 0] \to \mathbb{C}$ is of the form

$$F(\phi) = f(\phi(-\tau_1), \ldots, \phi(-\tau_n)),$$

or if F can be written as a point-wise limit of such functions.

Definition 2.2 (DDEs with state-dependent delay)**.** We say that the functional differential equation in (7) has a state-dependent delay if there exist functions $\tau_1, \ldots, \tau_n : \mathbb{C} \to [-\tau, 0]$ such that $F : C[-\tau, 0]$ is of the form

$$F(\phi) = f\big(\phi\big(- \tau_1(\phi(0))\big), \ldots, \phi\big(- \tau_n(\phi(0))\big)\big).$$

or if F can be written as a point-wise limit of such functions.

Remark 2.3. First, it should be noted that allowing for point-wise limits also allows for functions F which involve integrals over the delay. Integral type DDEs involving a a delay-kernel are often considered as the most general cases for linear DDEs. Second, it should be noted that these two types do not exhaust the set of delay equations. A well studied type of equation we ignored in this classification is the class of neutral-DDEs, where the derivative may also involve a delay. Furthermore, the delay could, instead of just depending on the current state $u_t(0)$ also depend on the whole history of u. In this paper, we shall only treat constant or state-dependent cases with one or two delays (in which case one of the delays will be zero).

In the case that F has only one constant delay, it is easy to see that initial value problems for such DDE's generally have a unique solution. For such a problem we can write

$$F(u_t) = f(u(t), u_t(-\tau)) = f(u(t), u(t - \tau)),$$

where $f : \mathbb{C}^2 \to \mathbb{C}$. This means that for any initial condition $\psi \in C[-\tau, 0]$ and any $t \in [0, \tau]$ our DDE becomes an non-autonomous ODE

$$u'(t) = f(u(t), \psi(t - \tau)).$$

Hence, for well-behaved functions f, the Picard–Lindelöf theorem guarantees the existence and uniqueness of solutions. If we have existence up to $t = \tau$ we can even repeat this process, by considering u on $[0, \tau]$ as the initial value, to show existence up to $t = 2\tau$ and so on. A similar result can be shown for DDEs with more discrete delays or autonomous DDEs with constant delays.

Remark 2.4. It should be noted that this technique only allows us to go "forward" in time. The backward's time problem for DDEs is in general not well-defined and in the case of state-dependent DDEs both the forward and backward may be ill-posed.

In order to think of DDEs as dynamical systems, we need to identify the phase-space. Since F depends on $u_t : [-\tau, 0] \to \mathbb{C}$, the natural choice for the phase-space is $\mathcal{C}_\tau := C[-\tau, 0]$.

A solution of (7) in the phase-space is therefore given by the time-dependent family of functions $u_t \in \mathcal{C}_\tau$, where $u_t(s) = u(t+s)$.

In order to consider our problem as a dynamical system, we now wish to arrive at an expression for $\frac{d}{dt}u_t$. Suppose we have some u_{t_0} for a fixed time t_0 and consider some small $\epsilon > 0$. Since $u_t(s) = u(t+s)$ for any $s \in [-\tau, 0]$, we should have that $u_{t_0+\epsilon}(s) = u_{t_0}(s+\epsilon)$ whenever $-\tau \leq s+\epsilon \leq 0$, hence we can write

$$u_{t_0+\epsilon}(s) = \begin{cases} u_{t_0}(s) + \displaystyle\int_{t_0+s}^{t_0+s+\epsilon} F(u_\sigma)d\sigma & \text{if } s+\epsilon \geq 0 \\ \\ u_{t_0}(s+\epsilon) & \text{if } s+\epsilon \leq 0. \end{cases}$$

Taking the limit $\frac{d}{dt}u_t = \lim_{\epsilon\to 0} \frac{u_{t+\epsilon}-u_t}{\epsilon}$ then means that

$$\frac{d}{dt}u_t(s) = \begin{cases} F(u_t) & \text{if } s = 0 \\ \frac{d}{ds}u_t(s) & \text{if } s < 0. \end{cases} \tag{8}$$

What we see is that if we want to express our DDE as a vector field on $\mathcal{C}_\tau$, then we have to make a distinction between how it acts on $u_t(0)$ and $u_t(s)$ for $s \in [-\tau, 0)$. This reformulation of the DDE as a flow on a function space is illustrated in Figure 4. To highlight this distinction, let us make the following definition.

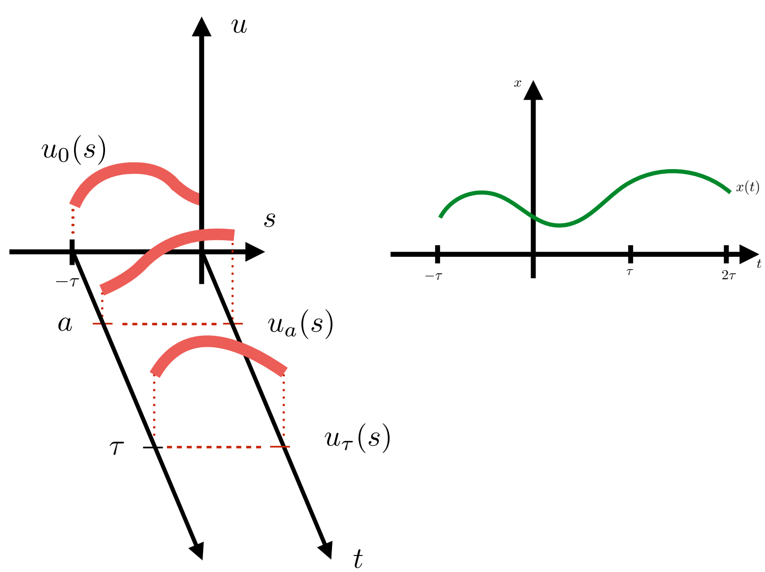

Figure 4: The phase space of a delay differential equation. The intuition is that we change to coordinates which “move with” the window of length τ.

Definition 2.5 (The discontinuous phase-space of a DDE)**.** Let $\mathcal{X}_\tau$ be the space of all functions on $[-\tau, 0]$ that are uniformly continuous on $[-\tau, 0)$ and that may posses a jump-discontinuity at $s = 0$. In notation:

$$\mathcal{X}_\tau := \mathbb{C} \times C_c([-\tau, 0)),$$

where $C_c([-\tau, 0))$ denotes the uniformly continuous functions on $[-\tau, 0)$. We define the norm in $\mathcal{X}_\tau$ by $\|(x, \psi)\| = \max\{|x|, \|\psi\|_\infty\}$. Since $C_c([-\tau, 0)) \cong C[-\tau, 0] = \mathcal{C}_\tau$, we can equivalently define

$$\mathcal{X}_\tau := \mathbb{C} \times \mathcal{C}_\tau.$$

We are, in the end, only interested in continuous solutions of (7), hence we will also introduce the following definition

Definition 2.6 (Classical solutions)**.** We call a pair $(x, \phi) \in \mathcal{X}_\tau$ *classical* if and only if $\psi(0) = x$. We denote the space of *classical* functions $\mathcal{X}_\tau^{\mathrm{cl}} \subset \mathcal{X}_\tau$ as

$$\mathcal{X}_\tau^{\mathrm{cl}} := \{(x, \psi) \in \mathcal{X}_\tau : \psi(0) = x\}.$$

It follows that we have a natural identification

$$\mathcal{X}_\tau^{\mathrm{cl}} \cong \mathcal{C}_\tau = C[-\tau, 0].$$

Inspired by (8), let us now consider the following ODE on $\mathcal{X}_\tau$:

$$\frac{d}{dt}\begin{pmatrix} u(t) \\ U_t \end{pmatrix} = \begin{pmatrix} F(u(t), U_t) \\ \frac{d}{ds}U_t \end{pmatrix}. \tag{9}$$

We can view the second equation in this system $\frac{d}{dt}U_t = \frac{d}{ds}U_t$ as a PDE on $[-\tau, 0] \times [0, \infty)$ and the method of characteristics tells us that any solution must be of the form

$$U_t(s) = \psi(t + s),$$

for all $s \in [-\tau, 0]$ and $t \in [0, \infty)$. This means that if we have a *classical* solution of (9), i.e., a solution that lies in $\mathcal{X}_\tau^{\mathrm{cl}}$ for all t, then we must have

$$U_t(s) = \psi(t + s) = U_{t+s}(0) = u(t + s),$$

or equivalently $u_t = U_t$ for all $t \in [\tau, 0)$. Hence $(u(t), U_t)$ is a classical solution of (9) if on only if $u(t)$ is a solution of (7).

This formalism now allows us to study DDEs as if they were ODEs on a Banach-space:

$$\frac{d}{dt}\mathcal{U}(t) = \mathcal{F}(\mathcal{U}(t)),$$

where $\mathcal{U}(t) = (u(t), U_t)$ and where $\mathcal{F} : \mathcal{X}_\tau \to \mathcal{X}_\tau$.

Definition 2.7. We shall call a map $\mathcal{F} : \mathcal{X}_\tau \to \mathcal{X}_\tau$ of *delay-type* whenever we can write

$$\mathcal{F}(x, \psi) = \begin{pmatrix} F(x, \psi) \\ \frac{d}{ds}\psi \end{pmatrix} \in \mathbb{C} \times \mathcal{C}_\tau.$$

for some function $F : \mathbb{C} \times \mathcal{C}_\tau \to \mathbb{C}$.

2.1.1 Equilibria and eigenvectors for delay equations

Let us consider now consider the ODE on a Banach space

$$\frac{d}{dt}\mathcal{U}(t) = \mathcal{F}(\mathcal{U}(t)), \tag{10}$$

where $\mathcal{F} : \mathcal{X}_\tau \to \mathcal{X}_\tau$ is of delay-type and recall that a point $(x, \psi) \in \mathcal{X}_\tau$ is an equilibrium if and only if $\mathcal{F}(x, \psi) = 0$. Since $\mathcal{F}$ is of delay-type, this in particular means that

$$\frac{d}{ds}\psi = 0,$$

so ψ must be a constant function. Furthermore, if (x, ψ) is also classical, then $\psi(0) = x$, hence $\psi(s) = x$ for all $s \in [0, \tau]$. Therefore all classical equilibria of (10) are simply constant functions in $\mathcal{X}_\tau^{\mathrm{cl}} = \mathcal{C}_\tau$ satisfying $F(x, \psi) = F(\psi(0), \psi) = 0$.

Remark 2.8. Of course the preceding result is not surprising. In the traditional formulation DDEs are written as

$$u'(t) = F(u_t),$$

hence it is immediately clear that u_t must be the same constant function for all t. However the result is a useful exercise in understanding the DDE/ODE formalism.

Suppose $\mathcal{U} \in \mathcal{X}_\tau$ is an equilibrium of $\mathcal{F}$, then we can write the linearized operator $D\mathcal{F}(\mathcal{U}) : \mathcal{X}_\tau \to \mathcal{X}_\tau$ as

$$D\mathcal{F}(\mathcal{U}) = \begin{pmatrix} D_x F(u, U) & D_\psi F(u, U) \\ 0 & \dfrac{d}{ds} \end{pmatrix}.$$

Suppose now that $(\xi, \Xi) \in \mathcal{X}_\tau$ is an eigenvector of $D\mathcal{F}(\mathcal{U})$ with eigenvalues λ, then

$$D\mathcal{F}(\mathcal{U}) \begin{pmatrix} \xi \\ \Xi \end{pmatrix} = \begin{pmatrix} D_x F(u, U)\xi + D_\psi F(u, U)\Xi \\ \frac{d}{ds}\Xi \end{pmatrix} = \lambda \begin{pmatrix} \xi \\ \Xi \end{pmatrix},$$

and $\frac{d}{ds}\Xi(s) = \lambda \Xi(s)$ for all $s \in [-\tau, 0]$, meaning that we can write

$$\Xi(s) = \Xi(0) e^{\lambda s}.$$

Since we are using this ODE representation to find solutions of DDEs, we are only interested in classical eigenfunctions of $D\mathcal{F}$, so we may assume that $\Xi(0) = \xi$, and indeed

$$\Xi(s) = \xi e^{\lambda s}.$$

Thus the eigenfunctions of $D\mathcal{F}$ are given by (scalar multiples of) the functions

$$\epsilon_\lambda(s) := e^{\lambda s}.$$

From this we have:

Lemma 2.9. *Let $\mathcal{U}$ be an equilibrium of $\mathcal{F}$, then $\lambda \in \mathbb{C}$ is a classical eigenvalue if and only if*

$$D_x F(\mathcal{U}) + D_\psi F(\mathcal{U}) \epsilon_\lambda = \lambda. \tag{11}$$

The corresponding eigenfunction is then given by $\epsilon_\lambda(s) := e^{\lambda s}$.

Example 2.10. Suppose that the function $F : \mathcal{X}_\tau \to \mathbb{C}$ is of the form

$$F(x, \psi) = f(x, \psi(-\tau))$$

and suppose that the equilibrium is given by the constant function $u = U(s) = c$ for all $s \in [-\tau, 0]$. Then (11) can be written as

$$\partial_1 f(c, c) + \partial_2 f(c, c)e^{-\lambda\tau} = \lambda. \tag{12}$$

Example 2.11. Suppose that the function $F : \mathcal{X}_\tau \to \mathbb{C}$ is of the (state-dependent) form

$$F(x, \psi) = f(x, \delta_{-\tau(x)}\psi) = f(x, \psi(-\tau(x))),$$

where $\delta_\alpha : \mathcal{C}_\tau \to \mathbb{C}$ given by $\delta_\alpha\phi = \phi(\alpha)$ is the Dirac-δ distribution at α. Furthermore, suppose that the equilibrium is given by the constant function $u = U(s) = c$ for all $s \in [-\tau, 0]$. We then have that

$$\begin{aligned} D_x F(x, \psi) &= D_x f(x, \psi(-\tau(x))) = \partial_1 f(x, \psi(-\tau(x))) - \partial_2 f(x, \psi(-\tau(x)))\phi'(-\tau(x))\tau'(x) \\ D_\psi F(x, \psi) &= D_\psi f(x, \delta_{-\tau(x)}\psi) = \partial_2 f(x, \delta_{-\tau(x)}\psi)\delta_{-\tau(x)}. \end{aligned}$$

Since our equilibrium must be a constant function, we find that $\phi' = U_t' = 0$, hence we find that (11) becomes identical to (12), namely

$$\partial_1 f(c, c) + \partial_2 f(c, c)e^{-\lambda\tau} = \lambda,$$

where in this case $\tau = \tau(c)$.

2.1.2 Periodic orbits and invariant vector bundles for delay equations

Let us now consider periodic solutions of (10). The problem of finding such solutions is greatly simplified if we pass to Fourier series, so suppose that we have coefficients $c_k \in \mathbb{C}$ and $C_k \in \mathcal{C}_\tau$, then we define $\mathcal{V} : [0, T] \to \mathcal{X}_\tau$ by

$$\mathcal{V}(\theta) = \begin{pmatrix} v(\theta) \\ V_\theta \end{pmatrix} = \begin{pmatrix} \displaystyle\sum_k c_k e^{ik\omega\theta} \\ \displaystyle\sum_k C_k e^{ik\omega\theta} \end{pmatrix},$$

where $\omega := 2\pi/T$. By a classical result of [58], we know that if the delay map is analytic, then a periodic solution of Equation (10) is analytic. Hence the Fourier coefficients of $\mathcal{V}$ decay exponentially fast.

If $\mathcal{V}$ is a periodic solution of (10), where $\mathcal{F}$ is of delay type, then clearly the second component must satisfy $\frac{\partial}{\partial\theta}V_\theta(s) = \frac{d}{ds}V_\theta(s)$, from which it follows that

$$\frac{\partial}{\partial\theta}\sum_k C_k(s)e^{ik\omega\theta} = \frac{d}{ds}\sum_k C_k(s)e^{ik\omega\theta},$$

or

$$i\omega\sum_k kC_k(s)e^{ik\omega\theta} = \sum_k C_k'(s)e^{ik\omega\theta}.$$

Isolating the Fourier coefficients, C_k satisfies

$$C_k'(s) = ik\omega C_k(s).$$

Imposing that $\mathcal{V}$ is a classical solutions of (10), it is immediately clear that $C_k(0) = c_k$, and therefore

$$C_k(s) = C_k(0)e^{ik\omega s} = c_k e^{ik\omega s}.$$

So,

$$V_\theta(s) = \sum_k C_k(s)e^{ik\omega\theta} = \sum_k c_k e^{ik\omega(s+\theta)}.$$

Summarizing: in order to find a periodic solution of (10), it suffices to solve

$$i\omega \sum_k k c_k e^{ik\omega\theta} = F\left(\sum_k c_k e^{ik\omega\theta}, \sum_k c_k e^{ik\omega(\bullet+\theta)}\right), \tag{13}$$

where $e^{ik\omega(\bullet+\theta)}$ denotes the map $s \mapsto e^{ik\omega(s+\theta)}$ for $s \in [-\tau, 0]$.

A numerical solution is obtained by truncating the Fourier series up to some order N, and computing zeros of the truncated function $\mathbb{R}^N \to \mathbb{R}^N$ via a Newton scheme. Since the period is a priori unknown we also treat it as a variable and fix a phase condition (like $v(0) = v^0$) to balance the system of equations.

Example 2.12. If the delay equation only has one delay, then Equation (13) becomes

$$i\omega \sum_k k c_k e^{ik\omega\theta} = f\left(\sum_k c_k e^{ik\omega\theta}, \sum_k c_k e^{ik\omega(\theta-\tau)}\right). \tag{14}$$

If f is polynomial then the right-hand-side is a linear combination of discrete convolutions of the coefficients c_k and $c_k e^{-ik\omega\tau}$.

Suppose now that $\mathcal{V}(\theta) = \binom{v(\theta)}{V_\theta}$ is a periodic solution of (10), of least period T. Then the vector bundle $\binom{\xi(\theta)}{\Xi_\theta} \in \mathcal{X}_\tau$, with $\theta \in [0, 2T]$, corresponding to the Floquet exponent λ satisfies

$$\frac{\partial}{\partial\theta}\begin{pmatrix}\xi(\theta)\\ \Xi_\theta\end{pmatrix} = \begin{pmatrix}D_x F(v(\theta), V_\theta)\xi(\theta) + D_\psi F(v(\theta), V_\theta)\Xi_\theta \\ \frac{d}{ds}\Xi_\theta\end{pmatrix} - \lambda\begin{pmatrix}\xi(\theta)\\ \Xi_\theta\end{pmatrix}. \tag{15}$$

Note that we parametrize the vector bundle over $[0, 2T]$ to account for the possibility that the Floquet multiplier is negative.

While (15) is an ODE on $\mathcal{X}_\tau$, we note that for $\lambda \neq 0$ it is *not* of delay type. However, we do know that for every $\theta \in [0, 2T]$

$$\frac{\partial}{\partial\theta}\Xi_\theta = \frac{d}{ds}\Xi_\theta - \lambda\Xi_\theta,$$

and hence by the method of characteristics we must have that

$$\Xi_\theta(s) = e^{\lambda s}\psi(\theta + s).$$

Defining $\binom{\hat{\xi}(\theta)}{\hat{\Xi}_\theta}$ by

$$\begin{aligned}\hat{\xi}(\theta) &= \xi(\theta)\\ \hat{\Xi}_\theta &= \epsilon_{-\lambda}\Xi_\theta,\end{aligned}$$

and then substituting this into Equation (15), we obtain

$$\frac{\partial}{\partial\theta}\begin{pmatrix}\hat{\xi}(\theta)\\ \hat{\Xi}_\theta\end{pmatrix}=\begin{pmatrix}(D_xF(v(\theta),V_\theta)-\lambda)\hat{\xi}(\theta)+D_\psi F(v(\theta),V_\theta)(\epsilon_\lambda\hat{\Xi}_\theta)\\ \frac{d}{ds}\hat{\Xi}_\theta\end{pmatrix}, \tag{16}$$

an equation of delay type. Furthermore it is clear that $\left(\begin{smallmatrix}\hat{\xi}(\theta)\\ \hat{\Xi}_\theta\end{smallmatrix}\right)$ is classical if and only if $\left(\begin{smallmatrix}\hat{\xi}(\theta)\\ \hat{\Xi}_\theta\end{smallmatrix}\right)$ is. Therefore, we reduce parametrizing the vector bundle of $\mathcal{V}$ to solving the DDE defined by (16).

Using this, and Equation (13), we simultaneously solve for the periodic solution (with Fourier coefficients c_k), the angular frequency of the vector bundle ($\omega/2=2\pi/2T$), the eigenfunction (with Fourier coefficients a_k) and the eigenvalue (λ) by solving the coupled system of equations

$$\begin{cases}\sum_k c_k=v^0\\ \sum_k a_k=\xi^0\\ \frac{1}{2}i\omega\sum_k kc_ke^{ik\omega\theta/2}=F\left(\sum_k c_ke^{ik\omega\theta/2},\sum_k c_ke^{ik\omega(\bullet+\theta)/2}\right)\\ \frac{1}{2}i\omega\sum_k ka_ke^{ik\omega\theta/2}=(D_xF(\dots)-\lambda)\sum_k a_ke^{ik\omega\theta/2}+D_\psi F(\dots)\sum_k ka_ke^{ik\omega(\bullet+\theta)/2}e^{\lambda\bullet},\end{cases} \tag{17}$$

where $F(\dots)$ is short for $F\left(\sum_k c_ke^{ik\omega\theta/2},\sum_k c_ke^{ik\omega(\bullet+\theta)/2}\right)$. Moreover, we reconstruct $\xi(\theta)$ and Ξ_θ by setting

$$\begin{aligned}\xi(\theta)&=\sum_k a_ke^{ik\omega\theta/2}\\ \Xi_\theta(s)&=\sum_k a_ke^{ik\omega(s+\theta)/2}e^{\lambda s}.\end{aligned}$$

One can also solve for multiple eigenvalues simultaneously by adding equations to (17) as appropriate, however we do not pursue the degenerate case in the present work.

Example 2.13. For a single delay, Equation (17) is

$$\begin{cases}\sum_k c_k=v^0\\ \sum_k a_k=\xi^0\\ \frac{1}{2}i\omega\sum_k kc_ke^{ik\omega\theta/2}=f\left(\sum_k c_ke^{ik\omega\theta/2},\sum_k c_ke^{ik\omega(\theta-\tau)/2}\right)\\ \frac{1}{2}i\omega\sum_k ka_ke^{ik\omega\theta/2}=(\partial_1f(\dots)-\lambda)\sum_k a_ke^{ik\omega\theta/2}+\partial_2f(\dots)\sum_k ka_ke^{ik\omega(\theta-\tau)/2}e^{-\lambda\tau}.\end{cases} \tag{18}$$

2.1.3 Visualization of the phase space: delay embedding coordinates

Since the phase space of the ODE induced by a delay differential equation is infinite dimensional, a natural question is "how best to visualize orbits in this phase space?" The question

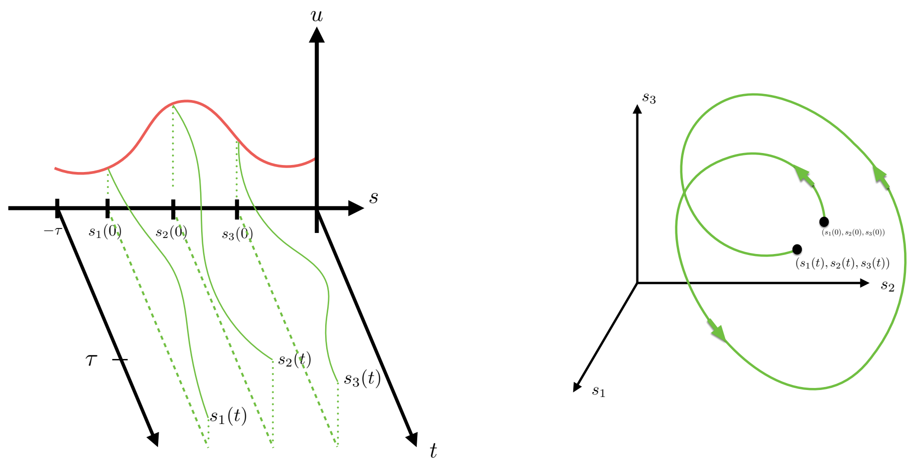

Figure 5: Left frame: solution of a delay equation with initial history segment colored in red. Right frame: solution of same delay equation with the evolution of the initial segment by time $t = a$ colored red.

is especially pertinent as in the present work we hope to visualize the invariant manifolds computed using the techniques developed below.

We use the classic notion of a delay embedding, see for example the works of [65, 59, 22, 69]. The idea is to think of the solution $x\colon \mathbb{R} \to \mathbb{R}$ of the delay equation as a time varying signal and embed $u(t)$ in $\mathbb{R}^n$ by choosing some numbers $0 \leq s_1 < \ldots < s_n \leq \tau$ and considering the shifted functions $u_1(t) = u(t - s_1)$, …, $u_n(t) = u(t - s_n)$ as our phase variables. Here $\tau > 0$ is the maximum delay associated with the DDE.

The notion is completely natural for delay equations. In fact when we think of the DDE as an ODE on the phase space $\mathcal{X}_\tau = C([-\tau, 0), \mathbb{R}) \times \mathbb{R}$ this idea leads to the following. With $-\tau \leq s_1 < \ldots < s_n \leq 0$ in $[-\tau, 0]$, suppose that $\mathcal{U} = (u(t), U_t(s))$ is a solution of Equation (10), with $\mathcal{U}_0 = (u(0), U_0(s))$ the initial condition. Consider as coordinates the functions

$$s_j(t) := U_t(s_j) \qquad\qquad 1 \leq j \leq n.$$

Then the curve $(s_1(t), \ldots, s_n(t))$ parameterizes an orbit in $\mathbb{R}^n$, and we take this as our projection.

Remark 2.14 (Three dimensional plotting)**.** In the present work we will always choose $s_1 = -\tau$, $s_2 = -\tau/2$, and $s_3 = 0$ unless specified otherwise. This provides a natural embedding of our systems into three dimensions and usually produces nice pictures.

3 The parameterization method

3.1 Unstable manifold attached to an equilibrium solution

Suppose that F is a (possibly unbounded) smooth vector field on the Banach space $\mathcal{X}$ and let $u^0 \in \mathcal{X}$ be a hyperbolic fixed point of F. Assume that F generates an (eventually) compact semiflow, which we denote by $\phi\colon \mathcal{X} \times \mathbb{R}^+ \to \mathcal{X}$. Then (since the semiflow is compact)

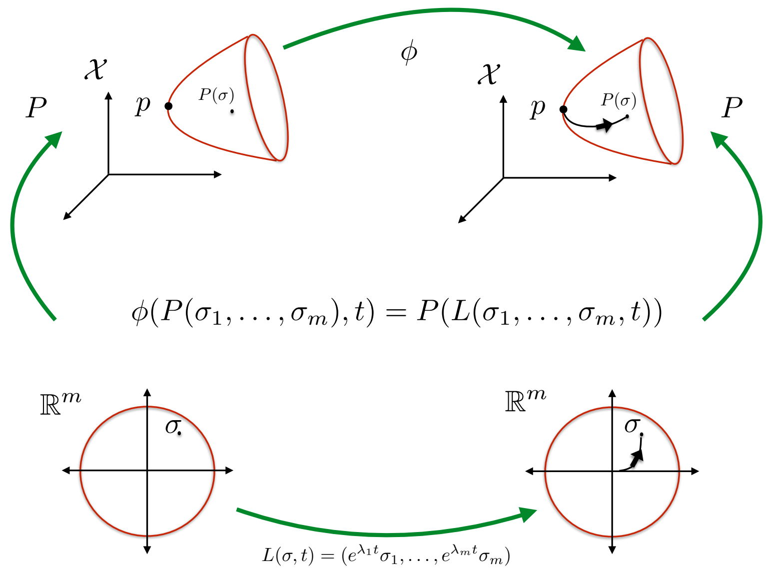

Figure 6: the dynamical meaning of the conjugacy described in Equation (20). The desired chart map conjugates the dynamics on the unstable manifold to the linear flow generated by the unstable eigenvalues.

the linear operator $DF(u^0)$ has only finitely many unstable eigenvalues (each with finite multiplicity) which we denote $\lambda_1, \ldots, \lambda_m \in \mathbb{C}$. We order the eigenvalues so that

$$0 < \mathrm{real}(\lambda_1) \leq \ldots \leq \mathrm{real}(\lambda_m).$$

For the sake of simplicity, we assume that each eigenvalue has multiplicity one. This is the only case which appears in the applications in the present work. More general cases can however be treated as discussed in [61]. Let $\xi_1, \ldots, \xi_m \in \mathcal{X}$ denote associated eigenvectors. Let

$$B^m := \{\sigma \in \mathbb{R}^m : \, |\sigma_j| < 1 \text{ for all } 1 \leq j \leq m\},$$

denote the unit cube in $\mathbb{R}^m$. The following definition is central.

Definition 3.1 (Conjugating chart map for a local unstable manifold of an equilibrium)**.** We say that a smooth map $P\colon B^m \to \mathcal{X}$ is a conjugating chart map for $W^u_{\mathrm{loc}}(u^0)$ if

$$P(0) = u^0, \qquad \frac{\partial}{\partial \sigma_j} P(0) = \xi_j, \tag{19}$$

for $1 \leq j \leq m$, and

$$\phi(P(\sigma_1, \ldots, \sigma_m), t) = P(e^{\lambda_1 t}\sigma_1, \ldots, e^{\lambda_m t}\sigma_m), \tag{20}$$

for all $(\sigma_1, \ldots, \sigma_m) \in B^m$ and $t \geq 0$ having that

$$(e^{\lambda_1 t}\sigma_1, \ldots, e^{\lambda_m t}\sigma_m) \in B^m.$$

The dynamical meaning of Equation (20) is illustrated in Figure 6.

Lemma 3.2. *Suppose that $P\colon B^m \to \mathcal{X}$ is a conjugating chart map in the sense of Definition 3.1. Then the image of P is a local unstable unstable manifold for u^0.*

Note that by simply reading the first order constraints given in Equation (19) we have that the image of P is an m-dimensional disk attached to u^0, and that the image of P is tangent at u^0 to the unstable eigenspace of $DF(u^0)$. Now, for $\sigma := (\sigma_1, \ldots, \sigma_m) \in B^m$ we note that the image of σ has a backward trajectory accumulating at the equilibrium u^0. To see this we define $x\colon (-\infty, 0] \to \mathcal{X}$ by

$$x(t) := P(e^{\lambda_1 t}\sigma_1, \ldots, e^{\lambda_m t}\sigma_m).$$

First we check that $x(t)$ is a backward orbit of $P(\sigma_1, \ldots, \sigma_m)$. Equation (20) then gives

$$\begin{aligned} \phi(x(-t), t) &= \phi(P(e^{-\lambda_1 t}\sigma_1, \ldots, e^{-\lambda_m t}\sigma_m), t) \\ &= P(e^{\lambda_1 t}e^{-\lambda_1 t}\sigma_1, \ldots, e^{\lambda_m t}e^{-\lambda_m t}\sigma_m) \\ &= P(\sigma_1, \ldots, \sigma_m), \end{aligned}$$

for any $t \in [0, \infty)$, i.e. any point on $x(t)$ with $t < 0$ flows to $x(0) = P(\sigma)$. Moreover, the backward orbit $x(t)$ accumulates at u^0, since

$$\begin{aligned} \lim_{t \to -\infty} x(t) &= \lim_{t \to -\infty} P(e^{\lambda_1 t}\sigma_1, \ldots, e^{\lambda_m t}\sigma_m) \\ &= P(0, \ldots, 0) \\ &= u^0 \end{aligned}$$

by the continuity of P and Equation (19).

The following proposition is the core of the parameterization method for an equilibrium solution.

Proposition 3.3 (Invariance equation: unstable manifold of a fixed point)**.** *Suppose that $P\colon B^m \to \mathcal{X}$ satisfies the linear constraints of Equation* (19)*, and that*

$$F[P(\sigma_1, \ldots, \sigma_m)] = \lambda_1\sigma_1\frac{\partial}{\partial\sigma_1}P(\sigma_1, \ldots, \sigma_m) + \ldots + \lambda_m\sigma_m\frac{\partial}{\partial\sigma_m}P(\sigma_1, \ldots, \sigma_m), \qquad (21)$$

for all $(\sigma_1, \ldots, \sigma_m) \in B^m$. Then P is a conjugating chart map in the sense of Definition 3.1, and hence the image of P is a local unstable manifold attached to u^0 by Lemma 3.2.

The proof follows (for example) by adapting the proof of Lemma 2.1 in [70] to the case of an unstable manifold for a semi-flow.

Remark 3.4. By introducing a little extra notation we obtain a convenient and abbreviated version of Equation (21). Define the $m \times m$ diagonal matrix of unstable eigenvalues

$$\Lambda = \left(\begin{array}{ccc} \lambda_1 & \ldots & 0 \\ \vdots & \ddots & \vdots \\ 0 & \ldots & \lambda_m \end{array} \right)$$

and let $\sigma = (\sigma_1, \ldots, \sigma_m)$. Then Equation (21) is equivalent to

$$F[P(\sigma)] = DP(\sigma)\Lambda\sigma. \qquad (22)$$

This sheds further light on Proposition 2.5, as geometrically speaking Equation (22) says that the push forward of the linear vector field Λ by P is tangent to (in fact equal to) the vector field F in the image of P. Then P carries orbits generated by Λ to orbits generated by F, i.e., we have an "infinitesimal conjugacy" between the vector field $\sigma' = \Lambda\sigma$ and vector field $x' = F(x)$ restricted to the image of P.

Remark 3.5 (Formal series solution and uniqueness)**.** As mentioned in the introduction, and illustrated explicitly for the case of DDEs in Section 4, a natural approach to solving Equation (21) is to develop formal series solutions. In fact this is the main topic of the original work of [4, 5, 6], where it is shown that the following notion of resonance provides the only obstruction to a formal series solution.

Definition 3.6 (Resonance of order α)**.** We say that the complex numbers $\lambda_1, \ldots, \lambda_m$ have a resonance of order $(\alpha_1, \ldots, \alpha_m) = \alpha \in \mathbb{N}^m$ if

$$\alpha_1\lambda_1 + \ldots + \alpha_m\lambda_m = \lambda_j,$$

for some $1 \leq j \leq m$ and some $|\alpha| \geq 2$. We say that $\lambda_1, \ldots, \lambda_m$ are non-resonant if there is no resonance of order α for any order $|\alpha| \geq 2$.

A central result of [4] is this: if the eigenvalues $\lambda_1, \ldots, \lambda_m$ are non-resonant, then for any choice of associated eigenvectors $\xi_1, \ldots, \xi_m$, there is a power series P which satisfies the linear constraints of Equation (19) and which solves Equation (21) in the sense of formal power series. Moreover the solution is unique up to the choice of the eigenvectors.

Since $\lambda_1, \ldots, \lambda_m$ are a finite collection of unstable eigenvalues there are only finitely many opportunities for resonances between these (as for $|\alpha|$ large enough the dot product on the left has magnitude larger than any of the finitely many unstable eigenvalues), i.e., despite first impressions, Definition 3.6 imposes only a finite number of constraints. For a more detailed discussion of this point see Lemma 4.2 and its proof in Section 4 of [54].

Remark 3.7 (A-priori convergence results)**.** Since the results described in Remark 3.5 give that a formal series solutions of Equation (21) exists as long as the eigenvalues are non-resonant in the sense of Definition 3.6, an important question is: does the formal series actually converge? In other words, do there exist analytic solutions of Equation (21)?

One answer to this question, which covers the case of present interest, is given by Theorem 3.2 of [60]. The theorem covers the case of an analytic, but unbounded, ordinary differential equation on a Banach space. Roughly speaking, the theorem says that if the eigenvalues are non-resonant then there exists a small enough choice of the scalings of the eigenvectors so that the formal series solution found by power matching actually converges on the m-dimensional unit poly-disk in $\mathbb{C}^m$. Note that Theorem 3.2 of [60] is stated for ODEs with sectorial linear part, but that the argument could be modified to cover unbounded linear operators associated with DDEs. What is actually needed is the variation of constants formula, and this formula can be recovered for retarded functional differential equations.

All that being said, in practice we are usually interested in large scalings of the eigenvectors as we would like to parameterize a large portion of the unstable manifold. In this case an a-priori result like the theorem just cited is useless to us. Instead, we are interested in developing a-posteriori analysis which can be used to validate the results of the parameterization method far from the fixed point. Such analysis is, for example, developed for PDEs in [60]. Extending the arguments of [60] to the cases studied in the present work, namely unstable manifolds of DDEs, will make the topic of an upcoming work.

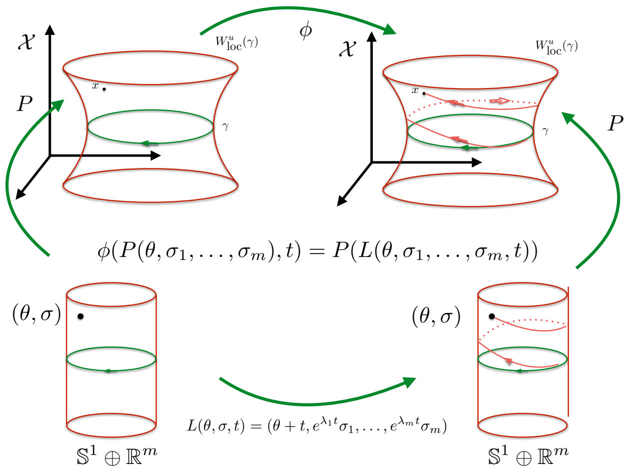

Figure 7: Unstable manifold of a periodic orbit γ.

3.2 Unstable manifold attached to a periodic solution

Let F be a (possibly unbounded) smooth vector field on the Banach space $\mathcal{X}$, $T > 0$, and suppose that $\gamma\colon [0,T] \to \mathcal{X}$ is a periodic orbit of least period T. Suppose in addition that γ has exactly m distinct unstable Floquet exponents $\lambda_1, \ldots, \lambda_m$ each of multiplicity one. Suppose that $\xi_1, \ldots, \xi_m\colon [0, 2T] \to \mathcal{X}$ are smooth periodic vector bundles parameterizing the unstable normal bundle of $\gamma(\theta)$. Note that $\xi_1, \ldots, \xi_m$ are allowed to have twice the period of the orbit to allow for the possibility that the bundles are non-orientable.

Definition 3.8 (Conjugating covering map for the local unstable manifold of a periodic orbit)**.** We say that a smooth map $P\colon [0,2T] \times B^m \to \mathcal{X}$ is a conjugating covering map for $W^u_{\text{loc}}(\gamma)$ if

$$P(\theta, 0) = \gamma(\theta), \qquad \frac{\partial}{\partial \sigma_j} P(\theta, 0) = \xi_j(\theta), \tag{23}$$

for all $1 \le j \le m$, and

$$\phi(P(\theta, \sigma_1, \ldots, \sigma_m), t) = P(\theta + t, e^{\lambda_1 t}\sigma_1, \ldots, e^{\lambda_m t}\sigma_m), \tag{24}$$

for all $t \ge 0$ such that

$$(e^{\lambda_1 t}\sigma_1, \ldots, e^{\lambda_m t}\sigma_m) \in B^m.$$

If P is a conjugating covering map in the sense of Definition 3.8 then the image of P is a local unstable manifold for γ. Justification of this claim is almost identical to the argument given after Lemma 3.2. A computationally convenient equivalent condition is given in the next proposition, which forms the core of the parameterization method for periodic orbits of differential equations. The proof for the case of finite dimensional vector fields is found in [11], and can be adapted to the present case of an unbounded ordinary differential equation densely defined on a Banach space.

Proposition 3.9 (Invariance equation: local unstable manifold for a periodic orbit)**.** *A smooth function $P\colon [0,2T] \times B^m \to \mathcal{X}$ is a conjugating covering map for a local unstable manifold if and only if P satisfies the linear constraints of Equation* (23) *and P solves the* *partial differential equation*

$$F[P(\theta,\sigma)] = \frac{\partial}{\partial\theta}P(\theta,\sigma) + \lambda_1\sigma_1\frac{\partial}{\partial\sigma_1}P(\theta,\sigma) + \ldots + \lambda_m\sigma_m\frac{\partial}{\partial\sigma_m}P(\theta,\sigma), \tag{25}$$

for all $\theta \in [0, 2T]$ *and all* $\sigma \in B^m$.

Remark 3.10 (A-priori existence)**.** One could establish a-priori existence for the periodic case in a manor similar to that discussed in Remark 3.7. The result is that a solution of Equation (25) exists and is unique (up to the scalings of the unstable vector bundles) as long as the non-resonance condition

$$\alpha_1\lambda_1 + \ldots + \alpha_m\lambda_m \neq \lambda_j, \qquad \text{for all } \alpha \in \mathbb{N}^M, \text{ and each } 1 \leq j \leq m,$$

holds between the Floquet exponents. Note that this is exactly the same notion of non-resonance which appears in the equilibrium case (see Definition 3.6) except with unstable eigenvalues replaced by unstable Floquet exponents. It also parallels the situation encountered when parameterizing local stable/unstable manifolds attached to periodic orbits of finite dimensional ODEs. See [6, 37, 37, 25, 11, 12] for further discussion.

4 Parameterization of Invariant Manifolds for Functional Differential Equations

We now adapt the theory of Section 3 to the specific case of an ODE associated with a delay differential equation (recall that this ODE formulation is reviewed in Section 2.1), and develop formal series solution solutions for Equations (21) and (25). In the following, we focus on the analytic case. However the case of finite differentiability is treated by stopping the procedure at lower order (see [4, 5]).

4.1 Unstable Manifold of an Equilibrium

Let $\lambda_1, \ldots, \lambda_m$ denote the unstable eigenvalues of an equilibrium solution $\mathcal{U}^0$, and $(\xi_j, \xi_j\epsilon_{\lambda_j}) \in \mathcal{X}_\tau^{\mathrm{cl}}$ denote a corresponding choice of eigenvectors. In fact we assume that each of the unstable eigenvalues has multiplicity one. To find a conjugating chart map $\mathcal{P} : B^m \to \mathcal{X}_\tau^{\mathrm{cl}}$ (in the sense of definition 3.1) we ask that

$$\mathcal{P}(0) = \mathcal{U}^0 \qquad\qquad \frac{\partial}{\partial\sigma_j}\mathcal{P}(0) = \begin{pmatrix} \xi_j \\ \xi_j\epsilon_{\lambda_j} \end{pmatrix},$$

and (by proposition 3.3) that

$$\mathcal{F}(\mathcal{P}(\sigma)) = D\mathcal{P}(\sigma)\Lambda\sigma, \tag{26}$$

where $\sigma \in \mathbb{R}^m$ and Λ is the diagonal matrix containing the unstable eigenvalues. Assuming $\mathcal{P}$ is analytic, we expand as a Taylor series. Using multi-index notation, write

$$\mathcal{P}(\sigma) = \sum_{|\beta|=0}^{\infty} \mathcal{P}_\beta \sigma^\beta,$$

where $\mathcal{P}_\beta \in \mathcal{X}_\tau$ for each multi-index β. In particular, this means that the right hand side of (26) is

$$D\mathcal{P}(\sigma)\Lambda\sigma = \sum_{|\beta|=0}^{\infty} (\lambda_1\beta_1 + \ldots + \lambda_m\beta_m)\sigma^\beta \mathcal{P}_\beta.$$

Write $\mathcal{P} = \left(\begin{smallmatrix} p \\ P \end{smallmatrix}\right)$, and consider separately the $\mathbb{C}$ and $\mathcal{C}_\tau$ components. Then we first rewrite (26) as

$$\begin{pmatrix} F(p(\sigma), P(\sigma)) \\ \dfrac{d}{ds}P(\sigma) \end{pmatrix} = \begin{pmatrix} Dp(\sigma)\Lambda\sigma \\ DP(\sigma)\Lambda\sigma \end{pmatrix},$$

and focus on the second component. Setting $\mathcal{P}_\beta = \left(\begin{smallmatrix} p_\beta \\ P_\beta \end{smallmatrix}\right)$, the left hand side of the second component is

$$\frac{d}{ds}P(\sigma) = \sum_{|\beta|=0}^{\infty} P_\beta \sigma^\beta = \sum_{|\beta|=0}^{\infty} \sigma^\beta \frac{d}{ds}P_\beta.$$

Combining with the right-hand side of (26), we have

$$\sum_{|\beta|=0}^{\infty} \sigma^\beta \frac{d}{ds}P_\beta(s) = \sum_{|\beta|=0}^{\infty} (\lambda\cdot\beta)\sigma^\beta P_\beta(s),$$

where $\lambda\cdot\beta = \lambda_1\beta_1 + \ldots + \lambda_m\beta_m$. Matching like powers yields

$$\frac{d}{ds}P_\beta(s) = (\lambda\cdot\beta)P_\beta(s),$$

from which we have

$$P_\beta(s) = P_\beta(0)e^{(\lambda\cdot\beta)s}.$$

Now imposing that the coefficients of $\mathcal{P}$ are classical (in the sense of definition 2.6) gives

$$P_\beta(s) = p_\beta e^{(\lambda\cdot\beta)s},$$

only i.e. $P_\beta = p_\beta \epsilon_{(\lambda\cdot\beta)}$. So: we have completely solved the $\mathcal{C}_\tau$-component of (26), and solving (26) is equivalent to finding all $p_\beta \in \mathbb{C}$ such that

$$F\left(\sum_{|\beta|=0}^{\infty} p_\beta\sigma^\beta, \sum_{|\beta|=0}^{\infty} \epsilon_{(\lambda\cdot\beta)} p_\beta \sigma^\beta\right) = \sum_{|\beta|=0}^{\infty} (\lambda\cdot\beta)\sigma^\beta p_\beta. \tag{27}$$

Since F is analytic, we expand as a power series. Substituting the power series for p and P into the power series for F leads to

$$F\left(\sum_{|\beta|=0}^{\infty} p_\beta\sigma^\beta, \sum_{|\beta|=0}^{\infty} \epsilon_{(\lambda\cdot\beta)} p_\beta \sigma^\beta\right) = \sum_{|\beta|=0}^{\infty} \left(p_\beta r_\beta + q_\beta\right)\sigma^\beta, \tag{28}$$

where q_β and r_β depend on p_γ with $|\gamma| < |\beta|$ only. Finally we iteratively solve (27) by computing q_β and r_β, and then solving for p_β in

$$p_\beta r_\beta + q_\beta = (\lambda\cdot\beta)p_\beta. \tag{29}$$

This method is summarized in algorithm 1. Of course in practice there remains some work to determine the form of r_β and q_β.

Algorithm 1 Unstable manifold of an equilibrium u^0

function PARAM_EUILIBRIUM($u^0; \xi_1, \dots, \xi_m; n_{\max}$)
  compute all distinct $\lambda_1, \dots, \lambda_m$ such that
    $D_x F(\mathcal{U}) + D_\psi F(\mathcal{U}) \epsilon_{\lambda_j} = \lambda_j$ ▷ the eigenfunctions are given by $\xi_j \epsilon_{\lambda_j}$
  $p_0 \leftarrow u^0$
  $p_{e_j} \leftarrow \xi_j$
  for all $n = 2$ to $n_{\max}$ **do**
    for all $|\beta| = m$ **do**
      compute q_β and r_β ▷ uses only p_γ with $|\gamma| < n$
      $p_\beta \leftarrow q_\beta / ((\lambda \cdot \beta) - r_\beta)$
    end for
  end for
  return $\{p_\beta\}_{0 \le |\beta| \le n_{\max}}$
end function

Example 4.1. Consider the special case where $F\colon \mathcal{X}_\tau \to \mathbb{C}$ comes from a DDE with a single constant delay $\tau > 0$, i.e.

$$F(x, \psi) = f(x, \psi(-\tau)),$$

with $f\colon \mathbb{C}^2 \to \mathbb{C}$ an analytic function. Then, taking another look at Equation (28), we would like to work out explicitly the form of r_β. To this end we write

$$\begin{aligned} F\left(\sum_{|\beta|=0}^{\infty} p_\beta \sigma^\beta, \sum_{|\beta|=0}^{\infty} \epsilon_{(\lambda\cdot\beta)} p_\beta \sigma^\beta\right) &= f\left(\sum_{|\beta|=0}^{\infty} p_\beta \sigma^\beta, \sum_{|\beta|=0}^{\infty} e^{-(\lambda\cdot\beta)\tau} p_\beta \sigma^\beta\right) \\ &= \sum_{|\beta|=0}^{\infty} s_\beta \sigma^\beta, \end{aligned}$$

where the power series coefficients $\{s_\beta\}_{\beta \in \mathbb{N}^m}$ are unknown. Define

$$p(\sigma) = \sum_{|\beta|=0}^{\infty} p_\beta \sigma^\beta, \qquad \text{and} \qquad \tilde{p}(\sigma) = \sum_{|\beta|=0}^{\infty} e^{-(\lambda\cdot\beta)\tau} p_\beta \sigma^\beta,$$

and note that, by Taylor's theorem

$$\frac{\partial^{|\beta|}}{\partial \sigma^\beta} p(0) = \beta!\, p_\beta, \qquad \text{and} \qquad \frac{\partial^{|\beta|}}{\partial \sigma^\beta} \tilde{p}(0) = \beta!\, e^{-(\lambda\cdot\beta)\tau} p_\beta.$$

Similarily,

$$s_\beta = \frac{1}{\beta!} \frac{\partial^{|\beta|}}{\partial \sigma^\beta} f(p(0), \tilde{p}(0)).$$

Applying the Faa Di Bruno Formula (see for example [13]) gives that

$$\frac{\partial^{|\beta|}}{\partial \sigma^\beta} f(p(\sigma), \tilde{p}(\sigma)) = \sum_{k=1}^{|\beta|} a_k D^k f(p(\sigma), \tilde{p}(\sigma))[\eta_1^\beta, \dots, \eta_k^\beta]$$

where a_k are some combinatorial coefficients, and the differential $D^k f$ is a k-th order symmetric tensor whose components are given by partial derivatives of f. Recalling that this is a generalization of the chain rule for multivariate functions, we see that the tensor is evaluated at vectors η_j^β, with $1 \leq j \leq k$, whose components are given by partial derivatives of various orders of the functions $p(\sigma)$ and $\tilde{p}(\sigma)$. The explicit form of the vectors η_j^β is not relevant to the current discussion. What matters for us is that the highest order partial derivatives, i.e. derivatives of order $|\beta|$, appear only in the $k = 1$ term, and in this case $D^k F$ is a rank one tensor, i.e. is the gradient of F. For $2 \leq k \leq |\beta|$ $D^k F$ is a rank k tensor, but the η_j^β involve partial derivatives of order strictly less than $|\beta|$. These observations allow us to write

$$\frac{\partial^{|\beta|}}{\partial \sigma^\beta} f(p(\sigma), \tilde{p}(\sigma)) = D^1 f(p(\sigma), \tilde{p}(\sigma)) \frac{\partial^{|\beta|}}{\partial \sigma^\beta} \begin{pmatrix} p(\sigma) \\ \tilde{p}(\sigma) \end{pmatrix} + \sum_{k=2}^{|\beta|} a_k D^k f(p(\sigma), \tilde{p}(\sigma))[\eta_1^\beta, \ldots, \eta_k^\beta],$$

where the remaining η_j^β depend only on partial derivatives of p and $\tilde{p}$ of order lower than $|\beta|$. Evaluating at zero leads to

$$\begin{aligned} \frac{\partial^{|\beta|}}{\partial \sigma^\beta} f(p(0), \tilde{p}(0)) &= D^1 f(p(0), \tilde{p}(0)) \frac{\partial^{|\beta|}}{\partial \sigma^\beta} \begin{pmatrix} p(0) \\ \tilde{p}(0) \end{pmatrix} + \sum_{k=2}^{|\beta|} a_k D^k f(p(0), \tilde{p}(0))[\eta_1^\beta(0), \ldots, \eta_k^\beta(0)] \\ &= \beta! \, \nabla f(c, c) \begin{pmatrix} p_\beta \\ e^{-(\lambda \cdot \beta)\tau} p_\beta \end{pmatrix} + q_\beta, \end{aligned}$$

where

$$q_\beta := \sum_{k=2}^{|\beta|} a_k D^k f(p(0), \tilde{p}(0))[\eta_1^\beta(0), \ldots, \eta_k^\beta(0)],$$

is a sum involving only p_δ with $|\delta| < |\beta|$. Interpreting this result in terms of Taylor series coefficients leads to

$$s_\beta = \left(\partial_1 f(c, c) + \partial_2 f(c, c) e^{-(\lambda \cdot \beta)\tau} \right) p_\beta + q_\beta,$$

which, since q_β depends only on terms of the form p_δ with $|\delta| < |\beta|$, gives explicitly the dependance of s_β on p_β. Returning to Equation (29), we now have

$$r_\beta = \partial_1 f(c, c) + \partial_2 f(c, c) e^{-(\lambda \cdot \beta)\tau},$$

and that in fact, the homological equations for the coefficients of $p(\sigma)$ are given by

$$\left(\partial_1 f(c, c) + \partial_2 f(c, c) e^{-(\lambda \cdot \beta)\tau} - (\lambda \cdot \beta) \right) p_\beta = -q_\beta. \tag{30}$$

This allows us to solve uniquely for p_β as long as

$$\partial_1 f(c, c) + \partial_2 f(c, c) e^{-(\lambda \cdot \beta)\tau} - (\lambda \cdot \beta) \neq 0.$$

Recalling the results from Example 2.10, this says that p_β is uniquely defined as long as $(\lambda \cdot \beta)$ is not equal to an eigenvalue, i.e. as long as $\lambda_1, \ldots, \lambda_m$ are non-resonant in the sense of Definition 3.6.

So, in addition to recovering the obstruction results described in Remark 3.5, we now know exactly the form of r_β for a large class of problems. (Similar results can be worked out for equations with multiple constant delays, or delays given by integrals). Having an explicit formula for r_β is useful for example when we implement Algorithm 1.

Note that the explicit form of q_β could also be worked out by considering more carefully the Faa Di Bruno Formula. However, this formula involves complicated combinatorial sums and in practice better results are obtained by applying the power matching scheme from scratch in applications. We illustrate this approach in several example problems below. In this case knowing in advance the form of r_β provides a useful check on our calculations.

4.1.1 Example: one dimensional unstable manifold in the cubic Ikeda equation

In numerical experiments the *cubic Ikeda equation*:

$$u'(t) = u(t-\tau) - u(t-\tau)^3, \tag{31}$$

with $1.538 \leq \tau \leq 1.723$ is a DDE that is known to exhibit chaotic behavior. In the discussion to follow we focus on $\tau = 1.59$. See for example the discussion in [67]. Rewriting Equation (31) as an ODE on the Banach Space $\mathcal{X}_\tau$ leads to

$$\frac{d}{dt}\begin{pmatrix} u(t) \\ U_t \end{pmatrix} = \begin{pmatrix} U_t(-\tau) - U_t(-\tau)^3 \\ \dfrac{d}{ds}U_t \end{pmatrix}. \tag{32}$$

One checks that Equation (32) has 3 equilibria, namely $u = 0$ and $u = \pm 1$. Writing $F(x, \psi) = \psi(-\tau) - \psi(-\tau)^3$, $D_x F = 0$ and

$$DF_\psi(0) = \delta_{-\tau} \qquad\qquad DF_\psi(\pm 1) = -2\delta_{-\tau},$$

where $\delta_\sigma : \mathcal{X}_\tau \to \mathbb{C}$, defined by $\delta_\sigma \psi = \psi(\sigma)$ is the Dirac-distribution at σ.

From lemma 2.9 it follows that all eigenvalues around $u = 0$ must satisfy

$$e^{-\lambda\tau} = \lambda.$$

When τ is in the chaotic regime, this equation has only one solution with real$(\lambda) > 0$.

Since there is exactly one unstable eigenvalue, the corresponding unstable manifold is 1-dimensional, and we write $\mathcal{P}(\sigma) = \sum_{k=0}^\infty \mathcal{P}_k \sigma^k$. Furthermore, since we are considering the equilibrium at 0, set

$$\mathcal{P}(0) = \mathcal{P}_0 = 0 \qquad\qquad \frac{\partial}{\partial\sigma}\mathcal{P}(0) = \mathcal{P}_1 = \xi^0 \epsilon_\lambda,$$

where $\xi^0 \in \mathbb{R}$ is a constant fixing the length and direction of the eigenvector.

Now note that

$$\begin{aligned} F\left(\sum_{k=0}^\infty p_k \sigma^k, \sum_{k=0}^\infty \epsilon_{\lambda k} p_k \sigma^k\right) &= \left(\sum_{k=0}^\infty e^{-\lambda k \tau} p_k \sigma^k\right) - \left(\sum_{k=0}^\infty e^{-\lambda k\tau} p_k \sigma^k\right)^3 \\ &= \sum_{k=0}^\infty e^{-\lambda k\tau} p_k \sigma^k - \sum_{k=0}^\infty e^{-\lambda k \tau}\sigma^k \sum_{\substack{k_1+k_2+k_3=k \\ k_1,k_2,k_3 \geq 0}} p_{k_1} p_{k_2} p_{k_3}. \end{aligned}$$

Substituting this into Equation (27) we find

$$\sum_{k=0}^\infty e^{-\lambda k\tau} p_k \sigma^k - \sum_{k=0}^\infty \sum_{\substack{k_1+k_2+k_3=k \\ k_1,k_2,k_3\geq 0}} e^{-\lambda k\tau} p_{k_1} p_{k_2} p_{k_3} \sigma^k = \sum_{k=0}^\infty k\lambda \sigma^k p_k,$$

and matching like powers of σ gives

$$e^{-\lambda k\tau}p_k - e^{-\lambda k\tau}\sum_{\substack{k_1+k_2+k_3=k\\ k_1,k_2,k_3\geq 0}} p_{k_1}p_{k_2}p_{k_3} = k\lambda p_k.$$

We now express p_k in terms of p_{k-1}, p_{k-2}, etc. Note that in the above Cauchy product p_k only appears when multiplied with $p_0 = 0$, i.e. the previous equation yields

$$p_k = \frac{e^{-\lambda k\tau}}{e^{-\lambda k\tau} - k\lambda}\sum_{\substack{k_1+k_2+k_3=k\\ 0\leq k_1,k_2,k_3<k}} p_{k_1}p_{k_2}p_{k_3}.$$

Alternatively, set

$$q_k = -e^{-\lambda k\tau}\sum_{\substack{k_1+k_2+k_3=k\\ 0\leq k_1,k_2,k_3<k}} p_{k_1}p_{k_2}p_{k_3} \qquad\qquad r_k = e^{-\lambda k\tau},$$

and compute p_k iteratively using algorithm 1.

4.1.2 Example: two dimensional unstable manifolds in the cubic Ikeda equation

In this section be reconsider briefly the example discussed in the introduction, since we can now make precise the formulas stated there. Consider the eigenvalues at $u = \pm 1$. In this case

$$DF_\psi(\pm 1) = -2\delta_{-\tau},$$

and by lemma 2.9 the eigenvalues are solutions of the equation

$$-2e^{-\lambda\tau} = \lambda.$$

When $\tau = 1.69$ the equation has exactly two complex conjugate solutions with real$(\lambda) > 0$, and the unstable manifold is two dimensional.

At the equilibrium ± 1 set

$$\mathcal{P}(0) = \mathcal{P}_0 = \pm 1 \qquad \frac{\partial}{\partial\sigma_1}\mathcal{P}(0) = \mathcal{P}_{10} = \xi^0\epsilon_{\lambda_-} \qquad \frac{\partial}{\partial\sigma_2}\mathcal{P}(0) = \mathcal{P}_{01} = \xi^0\epsilon_{\lambda_+},$$

where $\xi^0 \in \mathbb{R}$ is a constant fixing the length of the eigenvectors. Substituting $\mathcal{P}(\sigma) = \sum_{|\beta|=0}^\infty \mathcal{P}_\beta\sigma^\beta$ and $P_\beta = \epsilon_{(\lambda_-\beta_1+\lambda_+\beta_2)}p_\beta$, we find

$$F\left(\sum_{|\beta|=0}^\infty p_\beta\sigma^\beta, \sum_{|\beta|=0}^\infty P_\beta\sigma^\beta\right) = \sum_{k=0}^\infty e^{-\tau(\lambda\cdot\beta)}\left(p_k - \sum_{\substack{k_1+k_2+k_3=k\\ k_1,k_2,k_3\geq 0}} p_{k_1}p_{k_2}p_{k_3}\right)\sigma^k,$$

where $\lambda\cdot\beta = \lambda_-\beta_1 + \lambda_+\beta_2$. By substituting this into (27), and matching like powers of σ, we obtain

$$p_\beta = \frac{e^{-\tau(\lambda\cdot\beta)}}{(1-3p_{00}^2)e^{-\tau(\lambda\cdot\beta)} - (\lambda\cdot\beta)}\sum_{\substack{\gamma^1+\gamma^2+\gamma^3=\beta\\ |\gamma^i|<|\beta|}} p_{\gamma_1}p_{\gamma_2}p_{\gamma_3}.$$

We can also explicitly derive this result using algorithm 1, where we use as input, $p_{00} = \pm 1$ and $p_{01} = p_{10} = \xi^0$ and using

$$q_\beta = e^{-\tau(\lambda\cdot\beta)} \sum_{\substack{\gamma^1+\gamma^2+\gamma^3=\beta \\ |\gamma^i|<|\beta|}} p_{\gamma_1} p_{\gamma_2} p_{\gamma_3} \qquad\qquad r_\beta = e^{-\tau(\lambda\cdot\beta)}(1 - 3p_{00}^2).$$

4.1.3 Example: two dimensional unstable manifold in Wright's equation

Another commonly studied example is the famous Wright's equation, which is given by

$$u'(t) = -\alpha u(t-1)(1 + u(t)).$$

Here α is a positive parameter. Classic references for Wright's equation include the works of [73, 40, 41]. The equation has two equilibria, namely $u = 0$ and $u = -1$, and writing it as an ODE on a Banach space leads to

$$\frac{d}{dt}\begin{pmatrix} u(t) \\ U_t \end{pmatrix} = \begin{pmatrix} -\alpha U_t(-1)(1 + u(t)) \\ \dfrac{d}{ds}U_t \end{pmatrix}. \tag{33}$$

Let $F_\alpha(x, \psi) = -\alpha\psi(-1)(1 + x)$. Then it follows from lemma 2.9 that the eigenvalues around $u = -1$ satisfy

$$\alpha = \lambda,$$

hence $u = -1$ is a globally unstable equilibrium.

Around $u = 0$ on the other hand, we find that the eigenvalues satisfy

$$-\alpha e^{-\lambda} = \lambda,$$

an equation which has nontrivial solutions. In fact, the zero equilibrium undergoes a Hopf-bifurcation at $\alpha = \pi/2$, producing two (complex conjugate) unstable eigenvalues (which we denote λ_+ and λ_-), as well as a periodic solution. This periodic solution is conjectured to be the unique globally attracting slowly oscillating periodic solution. Indeed this is known as Wright's Conjecture, and we refer to [49, 48] for more complete discussion of recent progress on this conjecture.

Let us begin with the case where $\pi/2 < \alpha < 5\pi/2$. In this case, the equilibrium has exactly two unstable (complex conjugate) eigenvalues, which we denote by λ_+ and λ_-. Set

$$\mathcal{P}(0) = \mathcal{P}_{00} = 0 \qquad \frac{\partial}{\partial\sigma_1}\mathcal{P}(0) = \mathcal{P}_{10} = \xi^0\epsilon_{\lambda_-} \qquad \frac{\partial}{\partial\sigma_2}\mathcal{P}(0) = \mathcal{P}_{01} = \xi^0\epsilon_{\lambda_+},$$

where $\xi^0 \in \mathbb{R}$ is a (for the moment arbitrary) constant fixing the length of the eigenvectors.

Proceeding as before, we see that

$$F_\alpha\left(\sum_{|\beta|=0}^{\infty} p_\beta\sigma^\beta, \sum_{|\beta|=0}^{\infty} P_\beta\sigma^\beta\right) = -\alpha\sum_{|\beta|=0}^{\infty}\left(p_\beta e^{-\lambda\cdot\beta} + \sum_{\gamma^1+\gamma^2=\beta} p_{\gamma^1}p_{\gamma^2}e^{-\lambda\cdot\gamma^2}\right)\sigma^\beta,$$

where $\lambda\cdot\beta = \lambda_-\beta_1 + \lambda_+\beta_2$. Substituting this into (27), matching like powers of σ, and recalling that $p_{00} = 0$, we find

$$-\alpha p_\beta e^{-\lambda\cdot\beta} - \alpha\sum_{\substack{\gamma^1+\gamma^2=\beta \\ |\gamma^i|<|\beta|}} p_{\gamma^1}p_{\gamma^2}e^{-\lambda\cdot\gamma^2} = (\lambda\cdot\beta)p_\beta,$$

which we rewrite as

$$p_\beta = -\frac{\alpha}{(\lambda\cdot\beta)+\alpha e^{-\lambda\cdot\beta}} \sum_{\substack{\gamma^1+\gamma^2=\beta \\ |\gamma^i|<|\beta|}} p_{\gamma^1} p_{\gamma^2} e^{-\lambda\cdot\gamma^2}. \tag{34}$$

Alternatively, we apply algorithm 1, using

$$\begin{aligned} r_\beta &= -\alpha e^{-\lambda\cdot\beta} \\ q_\beta &= -\alpha \sum_{\substack{\gamma^1+\gamma^2=\beta \\ |\gamma^i|<|\beta|}} p_{\gamma^1} p_{\gamma^2} e^{-\lambda\cdot\gamma^2}. \end{aligned}$$

4.1.4 Example: four dimensional unstable manifold in Wright's equation

At $\alpha = \frac{5}{2}\pi$ the origin undergoes a second Hopf-bifurcation, resulting in two more unstable eigenvalues and a (hyperbolic) periodic orbit, and we now have two distinct pair of (complex conjugate) unstable eigenvalues. We say that the pair with larger real part are the *fast* eigenvalues $\lambda^f_\pm$, and the pair with smaller real part are the *slow* eigenvalues $\lambda^s_\pm$. All linear stability results from the previous section apply to the present case, in particular a result almost identical to Equation (34). The difference is that now we have $\lambda = (\lambda^f_+, \lambda^f_-, \lambda^s_+, \lambda^s_-)$ a 4 dimensional vector and all multi-indices are 4-tuples.

4.2 Unstable Manifold of a Periodic Orbit

Let $\mathcal{V}(t) = \binom{v}{V}$ be a periodic solution of (10) of period $T > 0$, with Floquet exponents, $\lambda_1, \dots, \lambda_m$. Let $\binom{\xi^j(\theta)}{\Xi^j_\theta}$ parameterize the unstable vector bundles. To find the conjugating covering map $\mathcal{P} : [0, 2T] \times B^m \to \mathcal{X}_\tau$ (in the sense of Definition 3.8) we fix

$$\mathcal{P}(\theta, 0) = \mathcal{V}(\theta) \qquad\qquad \frac{d}{d\sigma_j}\mathcal{P}(\theta, 0) = \begin{pmatrix} \xi_j(\theta) \\ (\Xi_j)_\theta \end{pmatrix}$$

and look for $\mathcal{P}$ satisfying

$$\mathcal{F}(\mathcal{P}(\theta,\sigma)) = \frac{\partial}{\partial\theta}\mathcal{P}(\theta,\sigma) + D_\sigma \mathcal{P}(\theta,\sigma)\Lambda\sigma. \tag{35}$$

Consider the Taylor expansion $\mathcal{P}(\theta,\sigma) = \sum_{|\beta|=0}^\infty \mathcal{P}_\beta(\theta)\sigma^\beta$, with $\mathcal{P}_\beta : [0, 2T] \to \mathcal{X}_\tau$ periodic functions. Splitting $\mathcal{P}$ into its components, we write Equation (35) as

$$\begin{pmatrix} F(p(\theta,\sigma), P(\theta,\sigma))) \\ \sum_{|\beta|=0}^\infty \sigma^\beta \frac{d}{ds} P_\beta(\theta) \end{pmatrix} = \begin{pmatrix} \sum_{|\beta|=0}^\infty \frac{\partial}{\partial\theta} p_\beta(\theta)\sigma^\beta \\ \sum_{|\beta|=0}^\infty \frac{\partial}{\partial\theta} P_\beta(\theta)\sigma^\beta \end{pmatrix} + \begin{pmatrix} \sum_{|\beta|=0}^\infty (\lambda\cdot\beta) p_\beta(\theta)\sigma^\beta \\ \sum_{|\beta|=0}^\infty (\lambda\cdot\beta) P_\beta(\theta)\sigma^\beta \end{pmatrix}.$$

Matching like powers of σ in the second component gives

$$\frac{d}{ds}P_\beta(\theta) = \frac{\partial}{\partial\theta}P_\beta(\theta) + (\lambda\cdot\beta)P_\beta(\theta).$$

Imposing that $\mathcal{P}$ is classical, and then applying the method of characteristics, leads to

$$P_\beta(\theta)[s] = e^{(\lambda\cdot\beta)s} p_\beta(\theta+s),$$

giving the $P(\theta)$ component of $\mathcal{P}(\theta)$ explicitly in terms of $p(\theta)$. It therefore suffices to solve

$$F\left(\sum_{|\beta|=0}^{\infty} p_\beta(\theta)\sigma^\beta, \sum_{|\beta|=0}^{\infty} \epsilon_{\lambda\cdot\beta} p_\beta(\theta+\bullet\ )\sigma^\beta\right) = \sum_{|\beta|=0}^{\infty} \frac{\partial}{\partial\theta} p_\beta(\theta)\sigma^\beta + \sum_{|\beta|=0}^{\infty} (\lambda\cdot\beta) p_\beta(\theta)\sigma^\beta, \quad (36)$$

where $p_\beta(\theta+\bullet\ )$ denotes the map $s \mapsto p_\beta(\theta+s)$ for $s \in [-\tau, 0]$. As we see in examples below, Equation (36) can often be written as an infinite system of delay equations with data periodic in θ.

Remark 4.2. From here on we assume that F only involves one delay (as in example 2.10). Analogous results for multiple delays are derived similarly.

Under the assumption that F only has one delay, we write the left-hand side as

$$\begin{aligned} F\Big(\sum_{|\beta|=0}^{\infty} p_\beta(\theta)\sigma^\beta, \sum_{|\beta|=0}^{\infty} \epsilon_{\lambda\cdot\beta} p_\beta(\theta+\bullet\ )\sigma^\beta\Big) &= f\left(\sum_{|\beta|=0}^{\infty} p_\beta(\theta)\sigma^\beta, \sum_{|\beta|=0}^{\infty} e^{-(\lambda\cdot\beta)\tau} p_\beta(\theta-\tau)\sigma^\beta\right) \\ &= \sum_{|\beta|=0}^{\infty} \big(p_\beta(\theta) r_\beta^0(\theta) + p_\beta(\theta-\tau) r_\beta^1(\theta) + q_\beta(\theta)\big)\sigma^\beta, \end{aligned}$$

where q_β and $r_{j,\beta}$ are functions that depend only on p_γ, with $|\gamma| < |\beta|$. From this we see that Equation (36) is a system of non-autonomous inhomogeneous linear DDEs:

$$p_\beta(\theta) r_\beta^0(\theta) + p_\beta(\theta-\tau) r_\beta^1(\theta) + q_\beta(\theta) = \frac{d}{d\theta} p_\beta(\theta) + (\lambda\cdot\beta) p_\beta(\theta). \quad (37)$$

Projecting onto a Fourier basis leads to

$$p_\beta(\theta) = \sum_k p_{\beta,k} e^{ik\omega\theta/2} \qquad q_\beta(\theta) = \sum_k q_{\beta,k} e^{ik\omega\theta/2} \qquad r_\beta^j(\theta) = \sum_k r_{\beta,k}^j e^{ik\omega\theta/2},$$

and we see that Equation (37) is

$$\sum_{k_1+k_2=k} p_{\beta,k_1}\left(r_{\beta,k_2}^0 + e^{-ik_1\omega\tau/2} r_{\beta,k_2}^1\right) + q_{\beta,k} = \frac{1}{2} ik\omega p_{\beta,k} + (\lambda\cdot\beta) p_{\beta,k}. \quad (38)$$

Truncating all Fourier series to order N, we have that Equation (38) is simply a linear problem on $\mathbb{C}^{2N+1}$, hence is easily solved by standard methods. This method is summarized in algorithm 2.

Remark 4.3 (Explicit form of $r_\beta(\theta)$ in the case of a single constant delay)**.** A computation similar to that of Example 4.1 shows the following: if $F\colon \mathcal{X}_\tau \to \mathbb{C}$ is given by

$$F(x, \psi) = f(x, \psi(-\tau)),$$

with $f\colon \mathbb{C}^2 \to \mathbb{C}$ an analytic function, then

$$r_\beta^0(\theta) = \partial_1 f(v(\theta), v(\theta-\tau))$$

Algorithm 2 Unstable manifold of a periodic orbit v up to N Fourier modes

function $\textsc{Param\_Per}(T; c_{-N}, \dots, c_N; \xi_1^0, \dots, \xi_m^0; n_{\max})$ $\quad \triangleright\ v(\theta) \approx \sum_{|k| \le N} c_k e^{ik\omega\theta/2}$
 compute $\lambda_1, \dots, \lambda_n$ and $\mathbf{a}_1, \dots, \mathbf{a}_m \in \mathbb{C}^{2N+1}$, where
  $\mathbf{a}_j = (a_{j,-N}, \dots, a_{j,N})$, are chosen such that
  $\xi_j(\theta) \approx \sum_{|k| \le N} a_{j,k} e^{ik\omega\theta/2}$, for $\theta \in [0, 2T]$ and
  ξ_j satisfies (18) (with $\xi_j(0) = \xi_j^0$).
 $\mathbf{p}_0 \leftarrow \mathbf{c} = (c_{-N}, \dots, c_N)$
 $\mathbf{p}_{e_j} \leftarrow \mathbf{a}_j$
 for all $n = 1$ to $n_{\max}$ **do**
  for all $|\beta| = n$ **do**
   compute $\mathbf{q}_\beta, \mathbf{r}_\beta^0, \mathbf{r}_\beta^1 \in \mathbb{C}^{2N+1}$ $\quad \triangleright$ uses only $\mathbf{p}_\gamma$ with $|\gamma| < n$
   compute the matrix A_β satisfying

$$[A_\beta \mathbf{p}_\beta]_k = \left(\frac{1}{2} ik\omega + (\lambda \cdot \beta)\right) p_{\beta,k} - \sum_{k_1+k_2=k} p_{\beta,k_1} \left(r^0_{\beta,k_2} + e^{-ik_1\omega\tau/2} r^1_{\beta,k_2}\right)$$

   $\mathbf{p}_\beta \leftarrow A_\beta^{-1} \mathbf{q}_\beta$ $\quad \triangleright$ Solve for $A\mathbf{p}_\beta = \mathbf{q}_\beta$
  end for
 end for
 return $\{\mathbf{p}_\beta\}_{0 \le |\beta| \le n_{\max}}$
end function

and

$$r^1_\beta(\theta) = \partial_2 f(v(\theta), v(\theta - \tau)) e^{-(\lambda \cdot \beta)\tau},$$

where $v(\theta)$ is the periodic orbit. So, the homological equations associated with a periodic orbit, in the case of a single constant delay, are

$$\begin{aligned} q_\beta(\theta) = {} & \frac{d}{d\theta} p_\beta(\theta) + (\lambda \cdot \beta) p_\beta(\theta) \\ & - \partial_1 f(v(\theta), v(\theta - \tau)) p_\beta(\theta) - \partial_2 f(v(\theta), v(\theta - \tau)) e^{-(\lambda \cdot \beta)\tau} p_\beta(\theta - \tau) \end{aligned} \tag{39}$$

with $q_\beta(\theta)$ depending only on terms $p_\delta(\theta)$ of order $|\delta| < |\beta|$. In practice it is better to work out the form of $q_\beta(\theta)$ from scratch, exploiting the structure of the problem at hand. But the calculation above verifies the claim made in the introduction; that the homological equations are linear delay differential equations with periodic data.

4.2.1 Example: one unstable Floquet exponent in the cubic Ikeda equation

As already remarked above, the cubic Ikeda equation exhibits chaotic dynamics, and it is reasonable to think that the equation admits (many) unstable periodic orbits. We focus on two numerically computed periodic orbits $\mathcal{V}_\pm$ of period $T \approx 12.91$ which appear to be the orbits of minimal period in the attractor. Numerical computation of the normal bundle, the details of which are described in Section 5, suggest that these orbits have exactly one unstable Floquet multiplier each and that the associated vector bundles are non-orientable.

We write $v(\theta) = \sum_k c_k e^{ik\omega\theta/2}$, and (using (14)) find the periodic solution by solving

$$\frac{1}{2} i\omega \sum_k k c_k e^{ik\omega\theta/2} = \sum_k c_k e^{ik\omega(\theta-\tau)/2} - \left(\sum_k c_k e^{ik\omega(\theta-\tau)/2}\right)^3.$$

Here we express $\mathcal{V}$ as a function of period $2T$, due to the fact that the vector bundles have period $2T$.

Expanding the products using discrete convolutions leads to

$$\frac{1}{2}ik\omega c_k = e^{-ik\omega\tau/2}\left(c_k - \sum_{k_1+k_2+k_3=k} c_{k_1}c_{k_2}c_{k_3}\right).$$

Similarly, by writing $\xi(\theta) = \sum_k a_k e^{ik\omega\theta/2}$, we solve for the parameterization of the vector bundle. Simultaneously solving the system

$$\begin{cases} \displaystyle\sum_k c_k = v^0 \\ \displaystyle\sum_k a_k = \xi^0 \\ \displaystyle\frac{1}{2}ik\omega c_k = e^{-ik\omega\tau/2}\left(c_k - \sum_{k_1+k_2+k_3=k} c_{k_1}c_{k_2}c_{k_3}\right) \\ \displaystyle\frac{1}{2}ik\omega a_k = -\lambda a_k + e^{-\lambda\tau}e^{-ik\omega\tau/2}\left(a_k - 3\sum_{k_1+k_2+k_3=k} c_{k_1}c_{k_2}a_{k_3}\right), \end{cases}$$

yields the periodic orbit, its period, its unstable Floquet exponent and its unstable normal bundle. Here we impose the phase condition $v(0) = v^0$ and the eigenvector scaling $\xi(0) = \xi^0$.

Now, to find the covering map $\mathcal{P}$ set

$$p_0(\theta) = v(\theta) \qquad\qquad p_1(\theta) = \xi(\theta),$$

and substitute Equation (32) into Equation (36). This gives

$$\sum_{k=0}^{\infty} \epsilon_{\lambda k}(-\tau)p_k(\theta-\tau)\sigma^k - \left(\sum_{k=0}^{\infty} \epsilon_{-\lambda k}(\tau)p_k(\theta-\tau)\sigma^k\right)^3 = \sum_{k=0}^{\infty} \frac{\partial}{\partial\theta}p_k(\theta)\sigma^k + \sum_{k=0}^{\infty} \lambda k p_k(\theta)\sigma^k.$$

Matching like powers of σ gives

$$e^{-\lambda k\tau}p_k(\theta-\tau) - e^{-\lambda k\tau}\sum_{k_1+k_2+k_3=k} p_{k_1}(\theta-\tau)p_{k_2}(\theta-\tau)p_{k_3}(\theta-\tau) = \frac{\partial}{\partial\theta}p_k(\theta) + \lambda k p_k(\theta).$$

In particular,

$$\begin{aligned} q_k(\theta) &= -e^{-\lambda k\tau}\sum_{\substack{k_1+k_2+k_3=k \\ k_1,k_2,k_3<k}} p_{k_1}(\theta-\tau)p_{k_2}(\theta-\tau)p_{k_3}(\theta-\tau) \\ r_k(\theta) &= e^{-\lambda k\tau}\left(1 - 3p_0(\theta-\tau)^2\right), \end{aligned}$$

and we obtain an equation of the form (37), namely

$$\frac{d}{d\theta}p_k(\theta) + \lambda k p_k(\theta) = r_k(\theta)p_k(\theta-\tau) + q_k(\theta).$$

This equation is solved iteratively via algorithm 2.

4.2.2 Example: two (complex conjugate) unstable Floquet exponents in Wright's equation

As we mentioned in Section 4.1.3 and Section 4.1.4, Wright's equation undergoes Hopf-bifurcations at $\alpha = \pi/2$ and $\alpha = 5\pi/2$. While the first bifurcation produces a globally attracting (slowly oscillating) periodic solution, the second bifurcation yields an unstable periodic solution whose period is less than 1. This unstable periodic orbit has two complex conjugate Floquet exponents and we consider now the parameterization of the associated local unstable manifold.

Again, write $v(\theta) = \sum_k c_k e^{ik\omega\theta/2}$, and simultaneously solve for the periodic orbit, its period, a Floquet exponent and its eigenfunction by considering the system of equations

$$\begin{cases} \sum_k c_k = v^0 \\ \sum_k a_k = \xi^0 \\ \frac{1}{2} ik\omega c_k = -\alpha c_k e^{-ik\omega\tau/2} - \alpha \sum_{k_1+k_2=k} c_{k_1} c_{k_2} e^{-ik_1\omega/2} \\ \frac{1}{2} ik\omega a_k = -\lambda a_k - \alpha a_k e^{-ik\omega/2} - \alpha \sum_{k_1+k_2=k} \left(a_{k_1} c_{k_2} + c_{k_1} a_{k_2}\right) e^{-ik_1\omega\tau/2}. \end{cases}$$

Here we impose the phase condition $v(0) = v^0$ and the eigenvector scaling $\xi(0) = \xi^0$.

We that the for the unstable periodic solution, the above system has two (complex conjugate) solutions, corresponding to two (complex conjugate) unstable Floquet multipliers $e^{\lambda_+ T}$ and $e^{\lambda_- T}$, corresponding eigenfunctions $\xi^{\pm}$. Set

$$p_{00}(\theta) = v(\theta) \qquad p_{10}(\theta) = \xi^+(\theta) \qquad p_{01} = \xi^-(\theta),$$

and substitute Equation (33) into Equation (36). If we denote $\lambda = (\lambda_+, \lambda_-)$, then matching like powers of σ leads to

$$-\alpha e^{-(\lambda\cdot\beta)} p_\beta(\theta-1) - \alpha \sum_{\substack{\gamma^1+\gamma^2=\beta \\ \gamma^1,\gamma^2\neq\beta}} e^{-(\lambda\cdot\gamma^1)} p_{\gamma^1}(\theta-1) p_{\gamma^2}(\theta) = \frac{\partial}{\partial\theta} p_\beta(\theta) + (\lambda\cdot\beta) p_\beta(\theta).$$

In particular, we have

$$\begin{aligned} q_\beta(\theta) &= -\alpha \sum_{\substack{\gamma^1+\gamma^2=\beta \\ \gamma^1,\gamma^2\neq\beta}} e^{-(\lambda\cdot\gamma^1)} p_{\gamma^1}(\theta-1) p_{\gamma^2}(\theta) \\ r^0_\beta(\theta) &= -\alpha p_{00}(\theta-1) \\ r^1_\beta(\theta) &= -\alpha e^{-(\lambda\cdot\beta)} \left(1 + p_{00}(\theta)\right), \end{aligned}$$

an equation of the form (37). This leads us to the following expression:

$$q_\beta(\theta) + r^0_\beta(\theta) p_\beta(\theta) + r^1_\beta(\theta) p_\beta(\theta-1) = \frac{d}{d\theta} p_\beta(\theta) + (\lambda\cdot\beta) p_\beta(\theta),$$

which we solve iteratively via algorithm 2.

4.3 Unstable Manifold of an Equilibrium for State Dependent Delays

The theory discussed in Section 4.1 is still, to some degree, applicable to the state dependent case. Although state-dependent problems may be ill-posed on any phase space $\mathcal{C}_\tau$, we will apply the formalism for the constant delay case. Justification of these computations, via mathematically rigorous a-posteriori analysis, will make the topic of a future work.

In the state dependent case we encounter the composition function

$$C(x, \phi) := \phi(-\tau + \kappa x),$$

and need the power-series expansion

$$C\left(\sum_{|\beta|=0}^{\infty} p_\beta \sigma^\beta, \sum_{|\beta|=0}^{\infty} \epsilon_{(\lambda\cdot\beta)} p_\beta \sigma^\beta\right) = \sum_{|\beta|=0}^{\infty} c_\beta \sigma^\beta,$$

i.e. we seek c_β such that

$$\sum_{|\beta|=0}^{\infty} c_\beta \sigma^\beta = \sum_{|\beta|=0}^{\infty} p_\beta \sigma^\beta e^{-\tau(\lambda\cdot\beta)} \exp\left(\kappa(\lambda\cdot\beta)\sum_{|\beta|=0}^{\infty} p_\beta \sigma^\beta\right).$$

In other words, the problem of composition reduces to composing the unknown function $p(\sigma)$ with the exponential map. We will develop a power-series expansion for

$$g_\beta(\sigma) := \exp\left(\kappa(\lambda\cdot\beta)p(\sigma)\right) = \sum_{|\gamma|=0}^{\infty} g_{\beta,\gamma}\sigma^\gamma,$$

which will allow us to write

$$\sum_{|\beta|=0}^{\infty} c_\beta \sigma^\beta = \sum_{|\beta|=0}^{\infty} p_\beta \sigma^\beta e^{-\tau(\lambda\cdot\beta)}\left(\sum_{|\gamma|=0}^{\infty} g_{\beta,\gamma}\sigma^\gamma\right) = \sum_{|\beta|=0}^{\infty}\sigma^\beta \sum_{\gamma^1+\gamma^2=\beta} p_{\gamma^1} e^{-\tau(\lambda\cdot\gamma^1)} g_{\gamma^1,\gamma^2}.$$

We then have that $c_0 = p_0$ and for $\beta \neq 0$,

$$\begin{aligned}
c_\beta &= \sum_{\gamma^1+\gamma^2=\beta} p_{\gamma^1} e^{-\tau(\lambda\cdot\gamma^1)} g_{\gamma^1,\gamma^2} \\
&= p_\beta e^{-\tau(\lambda\cdot\beta)} g_{\beta,0} + \sum_{\substack{\gamma^1+\gamma^2=\beta \\ \gamma^1,\gamma^2\neq 0}} p_{\gamma^1} e^{-\tau(\lambda\cdot\gamma^1)} g_{\gamma^1,\gamma^2}.
\end{aligned}$$

Consider the coefficients of g. First

$$\partial^{e_j} g_\beta(\sigma) = \kappa(\lambda\cdot\beta) g_\beta(\sigma)\partial^{e_j} p(\sigma),$$

and the multivariate form of the general Leibniz gives that for all $|\gamma| \geq 0$,

$$\begin{aligned}
\partial^{\gamma+e_j} g_\beta(\sigma) &= \kappa(\lambda\cdot\beta)\partial^\gamma(g_\beta(\sigma)\partial^{e_j}p(\sigma)) \\
&= \kappa(\lambda\cdot\beta)\sum_{\eta\leq\gamma}\binom{\gamma}{\eta}\partial^\eta g_\beta(\sigma)\partial^{\gamma-\eta+e_j}p(\sigma).
\end{aligned}$$

Combining this with the multivariate form of the Taylor theorem, we find that

$$c_{\beta,\gamma} = \partial^\gamma g_\beta(0)/\gamma!$$

and that $p_\gamma = \partial^\gamma p(0)/\gamma!$. Then

$$\begin{aligned} g_{\beta,\gamma+e_j} &= \frac{\kappa(\lambda\cdot\beta)}{(\gamma+e_j)!}\sum_{\eta\le\gamma}\binom{\gamma}{\eta}\eta! g_{\beta,\eta}(\gamma-\eta+e_j)! p_{\gamma-\eta+e_j} \\ &= \frac{\kappa(\lambda\cdot\beta)}{\gamma_j+1}\sum_{\substack{\eta^1+\eta^2=\gamma+e_j\\ \eta^2\neq 0}}(\eta^2)_j g_{\beta,\eta^1}p_{\eta^2}. \end{aligned}$$

In summary

$$g_{\beta,\gamma} = \frac{\kappa(\lambda\cdot\beta)}{\gamma_j}\sum_{\substack{\eta^1+\eta^2=\gamma\\ \eta^2\neq 0}}(\eta^2)_j g_{\beta,\eta^1}p_{\eta^2}, \tag{40}$$

where j is any index such that $\gamma_j \neq 0$. Note that $g_{\beta,\gamma}$ depends on those coefficients p_η for which $|\eta| \le |\gamma|$.

This not only provides us with an iterative expression for the coefficients of g_β, it also shows that the second term of the coefficients of the compositions,

$$c_\beta = p_\beta e^{-\tau(\lambda\cdot\beta)}g_{\beta,0} + \sum_{\substack{\gamma^1+\gamma^2=\beta\\ \gamma^1,\gamma^2\neq 0}} p_{\gamma^1}e^{-\tau(\lambda\cdot\gamma^1)}g_{\gamma^1,\gamma^2}, \tag{41}$$

depends only on those p_η for which $|\eta| < |\beta|$. Then, in many cases, we can still apply Algorithm 1; albeit with a more delicate expression for q_β and r_β.

4.3.1 Example: two dimensional unstable manifolds in a state-dependent perturbation of Wright's equation

Consider the state-dependent DDE defined by

$$u'(t) = -\alpha u(t-1+\epsilon u(t)) - \alpha u(t)u(t-1), \tag{42}$$

where α is a positive parameter and where we start by thinking of $|\epsilon|$ as small. When $\epsilon = 0$, Equation (42) is Wright's equation. We can consider (42) as a state-dependent perturbation of Wright's equation and analyze the equilibria $u = 0$ and $u = -1$.

Using the ODE formalism, we can alternatively write (42) as

$$\frac{d}{dt}\begin{pmatrix} u(t) \\ U_t \end{pmatrix} = \begin{pmatrix} -\alpha U_t(-1+\epsilon u(t)) - \alpha u(t)U_t(-1), \\ \dfrac{d}{ds}U_t \end{pmatrix}. \tag{43}$$

Let $F(x,\phi) = -\alpha\phi(-1+\epsilon x) - \alpha x\phi(-1)$. Then (using example 2.11) we see that the eigenvalues satisfy

$$-\alpha e^{-\lambda} = \lambda,$$

an equation independent of ϵ. Then Equation (42) has exactly the same eigenvalues as the traditional Wright's equation. It follows that for $\pi/2 < \alpha < 5\pi/2$ we still find two unstable eigenvalues, which we denote by λ_+ and λ_-.

We hope to parametrize a 2-dimensional unstable manifold at this equilibrium, and set

$$\mathcal{P}(0) = \mathcal{P}_0 = 0 \qquad \frac{\partial}{\partial \sigma_1}\mathcal{P}(0) = \mathcal{P}_{10} = \xi^0 \epsilon_{\lambda_-} \qquad \frac{\partial}{\partial \sigma_2}\mathcal{P}(0) = \mathcal{P}_{01} = \xi^0 \epsilon_{\lambda_+},$$

where $\xi^0 \in \mathbb{R}$ is a constant fixing the length of the eigenvectors.

Consider the left hand side of (27). We have

$$F\left(p(\sigma), P(\sigma)\right) = -\alpha \sum_{|\beta|=0}^{\infty} p_\beta \sigma^\beta e^{(\lambda\cdot\beta)(-1+\epsilon p(\sigma))} - \alpha \sum_{|\beta|=0}^{\infty} \sigma^\beta \sum_{\gamma^1+\gamma^2=\beta} p_{\gamma^1} p_{\gamma^2} e^{-(\lambda\cdot\gamma^1)}.$$

Define $g_\beta(\sigma) = \exp(\epsilon(\lambda\cdot\beta)p(\sigma)) = \sum_{|\gamma|=0}^{\infty} g_{\beta,\gamma}\sigma^\gamma$ and, using the expression from Equation (41), we see that the invariance equation (given in (27)) becomes

$$-\alpha \sum_{|\beta|=0}^{\infty} \sigma^\beta \sum_{\gamma^1+\gamma^2=\beta} p_{\gamma^1} e^{-(\lambda\cdot\gamma^1)} \left(g_{\gamma^1,\gamma^2} + p_{\gamma^2}\right) = \sum_{|\beta|=0}^{\infty} (\lambda\cdot\beta) p_\beta \sigma^\beta.$$

Then matching like powers of σ leads to

$$-\alpha \sum_{\gamma^1+\gamma^2=\beta} p_{\gamma^1} e^{-(\lambda\cdot\gamma^1)} \left(g_{\gamma^1,\gamma^2} + p_{\gamma^2}\right) = (\lambda\cdot\beta) p_\beta.$$

Isolating p_β, and using the fact that $p_0 = 0$ (and hence $g_\beta(0) = 1$) we obtain

$$-\alpha p_\beta e^{-(\lambda\cdot\beta)} - \alpha \sum_{\substack{\gamma^1+\gamma^2=\beta \\ \gamma^1,\gamma^2\neq 0}} p_{\gamma^1} e^{-(\lambda\cdot\gamma^1)} \left(g_{\gamma^1,\gamma^2} + p_{\gamma^2}\right) = (\lambda\cdot\beta) p_\beta.$$

The second term in the left-hand side only depends on p_γ with $|\gamma| < |\beta|$, which allows us to iteratively solve for p_β.

In particular, if setting

$$\begin{aligned} r_\beta &= -\alpha e^{-(\lambda\cdot\beta)} \\ q_\beta &= -\alpha \sum_{\substack{\gamma^1+\gamma^2=\beta \\ \gamma^1,\gamma^2\neq 0}} p_{\gamma^1} e^{-(\lambda\cdot\gamma^1)} \left(g_{\gamma^1,\gamma^2} + p_{\gamma^2}\right), \end{aligned}$$

we solve for p_β by direct application of algorithm 1.

5 Numerical applications

5.1 Computation of eigendata

Algorithm 1, describing the computation of the unstable manifold of an equilibrium, relies on two pieces of initial data: namely the equilibrium itself and eigendata. Due to lemma 2.9 we can, in our examples, find the eigenfunctions and eigenvalues by solving an equation of the form

$$a + be^{-\lambda\tau} = \lambda. \tag{44}$$

The well known solutions of such transcendental characteristic equations are given by

$$\lambda = \frac{1}{\tau} W_k(b\tau e^{-a\tau}) + a,$$

where W_k denotes the k-th branch of the Lambert-W function. Then any numerical implementation of the Lambert-W function produces the eigenvalues of an equilibrium. Or, if so desired, one can solve Equation (44) using Newton's method. (This is an especially attractive option if validated numerical results are desired).

Likewise, algorithm 2 for computing the unstable manifold of a periodic solution relies on an accurate computation of the unstable eigenbundle, which requires that we solve the system described in (17). However, while it is relatively easy to compute the number of unstable eigenvalues in the case of an equilibrium, determining the number of unstable Floquet multipliers of a periodic solution is less straightforward. Finding a suitable starting point for a Newton scheme for solving Equation (17) is challenging in practice. We obtain a suitable starting point for the Newton iteration using techniques similar to those of [47, 24], and we refer to the work just cited for more complete discussion. Below we only sketch the method.

We determine the number of unstable eigenvalues, and their approximate values, by computing an approximation of the monodromy operator $M(T)$ associated with the periodic orbit. Likewise, we construct approximations of the eigenfunctions by looking at the eigenvectors of the approximation of $M(T)$. We construct this approximation of $M(T)$ as an operator on the n-dimensional subspace $S_n \subset C[-\tau, 0]$ of continuous piecewise linear functions (splines) with their base-points in a uniform grid of n points. (We choose to work with splines because these can be made to interact nicely with our DDE integrator of choice, dde23).

By taking an initial history in $S_n \cong \mathbb{R}^n$ and numerically integrating this, we approximate the Poincaré map on $\mathbb{R}^n$ near a previously computed periodic solution. The approximation of the monodromy operator is then given by the derivative of this Poncaré map. The eigenvalues of this derivative approximate the Floquet multipliers of the periodic solution of the DDE, and the eigenvectors provide a spline-approximation of the eigenfunctions corresponding to the periodic solution. Taking the FFT gives initial data for the Newton scheme in Fourier space.

5.2 Decay rates and Scaling

Besides the detailed eigendata that we covered above, algorithms 1 and 2 rely on one more piece of data, namely the scaling of the eigenfunctions. Since a scalar multiple of an eigenvector remains an eigenfuncton, the question remains: which scaling produces the "optimal" parametrization?

Since we know that the conjugating charts describing the unstable manifolds are analytic, we know that the Taylor coefficients of these charts decay exponentially. This means that, after computing enough terms, we will wind up with coefficients that are smaller than the machine-epsilon. It is clear that once this point has been reached, further computation is no longer meaningful. Since the conjugating charts are given by power series (with decay coefficients), we can a priori expect these to hold well at least on the unit ball.

This opens the door to our means of choosing the scaling. Namely, as is evident from the algorithms, choosing a larger scaling will result in larger coefficients. Therefore when given a fixed number of coefficients, we can simply choose our scaling such that the last coefficients are of machine precision. This will allow us to cover a part of the unstable manifold that is as large as possible while restricting the domain of the chart to the unit ball. Numerical algorithms for adaptively choosing the eigenvector scalings are discussed in detail in [2].

5.3 Benchmarks

In the remainder of this section, we discuss numerical results for examples developed in 4. To compare our results, we will, for all of the examples in 4, explicitly check the conjugacy relations covered in definitions 3.1 and 3.8. The conjugacy is checked via numerical integration.

In particular, after choosing an arbitrary initial point $\sigma^0 \in B^m$, we compare $u_i^1 := \phi(P(\sigma^0), \tau)$ and $u_p^1 := P(e^{\Lambda\tau}\sigma^0)$, i.e., we check how well the conjugacy holds after flowing an amount of time forward equal to the (maximum) delay of the DDE.

In these examples we choose our initial σ^0 in such a way that after applying the linear conjugation, we remain in the unit ball, but relatively close to the boundary. That is, we choose σ^0 such that $|e^{\Lambda\tau}\sigma^0| \approx 0.9$.

Given $u^0 := P(\sigma^0) \in \mathcal{C}_\tau$ we then calculate $u_i^1 = 1$ using the Matlab integrator dde23, in the case of constant delay, and ddesd for the state-dependent case. In either case, we use a relative tolerance of 10^{-9} and an absolute tolerance of 10^{-11}, which in each of these cases results in a solution comprised of approximately 10^3 integration steps.

Finally, in order to evaluate the polynomial P we use specially modified version of Horner's algorithm that incorporates the many exponentials (of the form $e^{\lambda\cdot\beta}$) to be evaluated.

The final defect is obtained by comparing the resulting $\mathcal{C}_\tau$ functions in the L^2 norm. Since the numerical integration (in each of the considered cases) uses approximately a thousand integration steps and has a relative tolerance of 10^-9, we can expect a defect in the numerical integration of approximately 10^{-6}. Hence if the parametrization is (at least) as accurate as the numerical integrator, we also expect the difference between the two $\mathcal{C}_\tau$ functions to be of the order of 10^{-6}.

5.4 Unstable manifolds of the cubic Ikeda equation

In the following subsections we shall calculate several unstable manifolds related to the cubic Ikeda equation. To provide the resulting pictures with a little more context, we have also computed a rough estimation of the chaotic attractor of the cubic Ikeda system, shown in figure 8. This was done by picking a point on the unstable manifold of the origin and integrating for roughly a thousand time steps.

5.4.1 1D unstable manifold through the equilibrium $u = 0$.

For $\tau = 1.59$ the linearized cubic Ikeda equation at the origin has exactly one unstable direction, with corresponding eigenvalue

$$\lambda = \frac{1}{\tau} W_0(\tau) \approx 0.47208.$$

We parametrize the unstable manifold to polynomial order 120, i.e. we use 121 Taylor coefficients. For the scaling we choose the eigenfunction $\xi^0 e^{\lambda s}$ with $\xi^0 = 27.0$. The resulting manifold is plotted in figure 8. The restricting factor in this computation is given by the amount of precision that can be attained in the computation of the coefficients. As can bee seen in figure 9, the largest coefficient in this scaling is already of the order of 10^8, meaning that evaluating with the normal machine precision of 10^{-16} this polynomial can only be

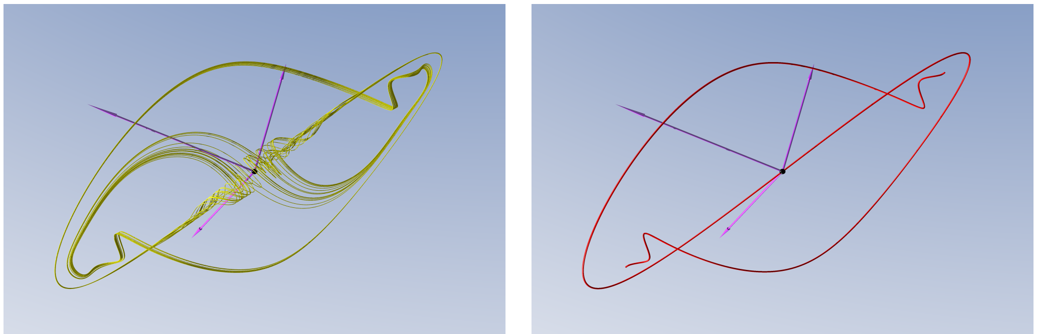

Figure 8: The attractor (yellow) and the unstable manifold (red) of the cubic Ikeda equation at $u = 0$. The attractor is computed simply by integrating arbitrary initial conditions using a standard DDE integrator. The unstable manifold is obtained by plotting the parameterization computed to 120 terms. Note that the parameterization captures several turns in the manifold, i.e. is far from the linear approximation (is not for example the graph of any function). The parameterization turns several times quite sharply near the ends.

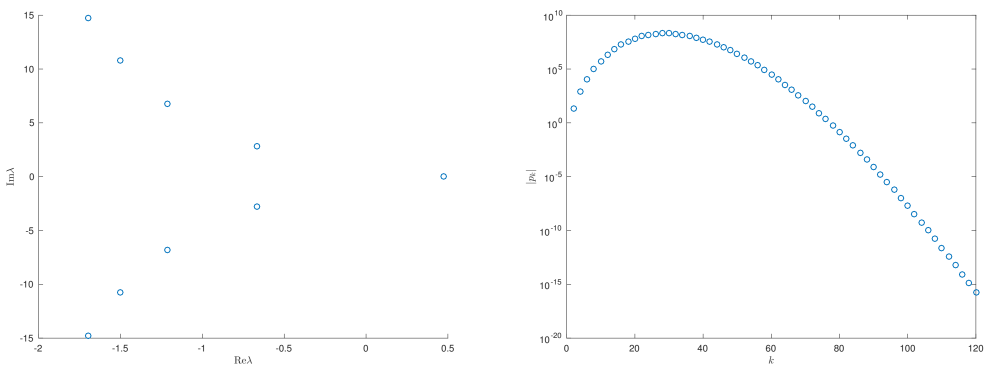

Figure 9: Left frame: the first 9 eigenvalues of the linearized cubic Ikeda equation at the origin. Right frame: the decay of the coefficients of the parametrization of the unstable manifold at $u = 0$.

done with a precision up to 10^{-8}. These results could therefore be significantly improved by making use of multiple-precision software. Using $u^0 = P(0.45)$, we find that

$$\|u_p^1 - u_i^1\|_2 \approx 9.25 \times 10^{-7}.$$

Not only does this lie within the expected error of the numerical integrator, but the resulting manifold actually captures a lot of interesting behaviour. This can readily bee seen from figure 11, where several clear bends following the attractor can be observed.

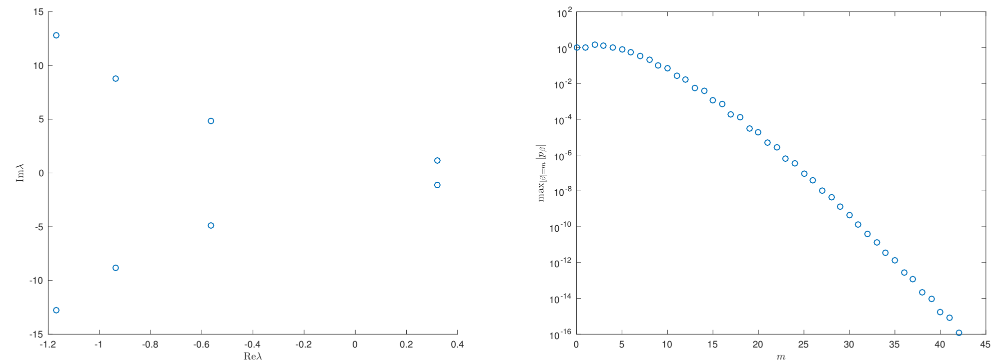

Figure 10: Left frame: the first 8 eigenvalues of the linearized cubic Ikeda equation at the points $u = \pm 1$. Right frame: the decay of the coefficients of the parametrization of the unstable manifolds at $u = \pm 1$.

5.4.2 2D Unstable manifold of the equilibrium $u = \pm 1$.

For $\tau = 1.59$ the linearized cubic Ikeda equation at the equlibria $u = \pm 1$ has exactly two unstable directions, with corresponding (complex conjugate) eigenvalues

$$\lambda_+ = \frac{1}{\tau} W_0(-2\tau) \approx 0.32056 + 1.15780$$
$$\lambda_- = \frac{1}{\tau} W_0(-2\tau) \approx 0.32056 - 1.15780.$$

We parametrize the unstable manifold to polynomial order 42, i.e. we use $43 \times 43 = 1849$ Taylor coefficients, shown in figure 10. Since the eigenvalues are complex conjugates, we choose the same scaling for both eigenfunctions, namely the eigenfunctions are given by $\xi^0 e^{\lambda_\pm s}$, where $\xi^0 = 0.95$.

Even though the eigenvalues, and also the coefficients produced by algorithm 1, are complex, we still realize the manifold as a real-valued manifold in $\mathcal{C}_\tau$. In fact, one easily checks that the coefficients of P are complex conjugate. Then the map $z \mapsto P(z, \overline{z})$ maps the complex (2-dimensional) unit disk in $\mathbb{C}$ to a real-valued image in $\mathcal{C}_\tau$. The resulting manifold is illustrated in figure 11. Use of complex conjugate coordinates to obtain real images with the parameterization method is discussed in more detail in [53, 50]. Using $u^0 = P(0.25 + 0.3i, 0.25 - 0.3i)$, we find that the defect of the conjugacy is

$$\|u_p^1 - u_i^1\|_2 \approx 2.79 \times 10^{-6}.$$

5.4.3 2D Unstable manifold of two periodic orbits.

We consider the two minimal periodic orbits of period $T \approx 12.91003$ illustrated in figure 13. These periodic orbits, each of which is simply the negative of the other, have one unstable Floquet multiplier approximately equal to -3.85. Using this, we then find that the corresponding real Floquet exponent is given by

$$\lambda \approx 0.10452.$$

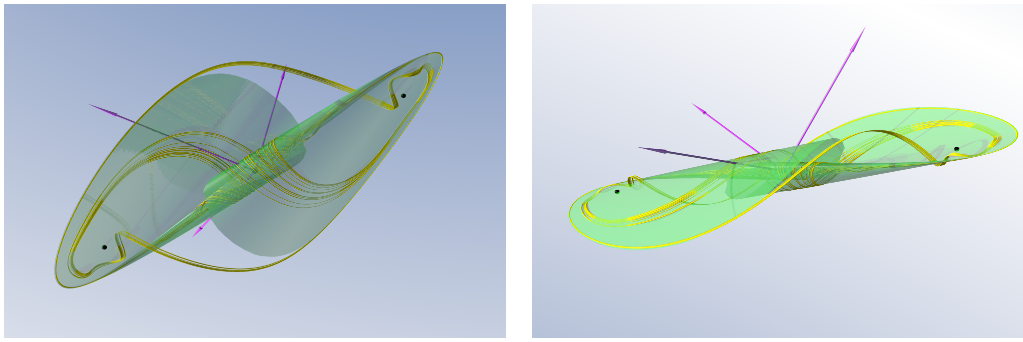

Figure 11: The equilibria (black dots), attractor (yellow) and two-dimensional manifolds at $u = \pm 1$ (green) as seen from two different angles. Note how these two manifolds wrap closely around each other near the origin.

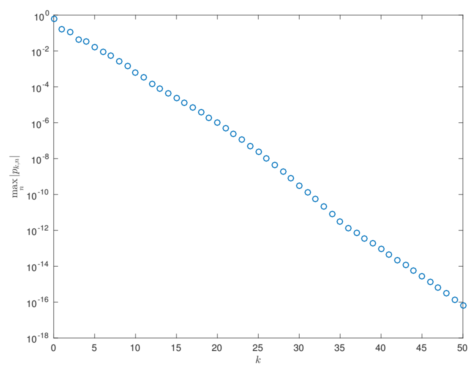

Figure 12: The decay of the coefficients of the parametrization of the unstable manifold of the minimal periodic solutions of the cubic Ikeda equation.

In this example we parametrize the unstable manifold to 50th order and employ 140 Fourier modes, using $51 \times (2 \times 140 + 1) = 14331$ Fourier-Taylor coefficients. The decay of these coefficients is shown in figure 12. For the scaling, we choose the eigenfunction ξ such that $\|\xi\|_2 = 0.31$, where we use the ℓ^2 norm on the space of Fourier-coefficients. Note that since the Floquet multiplier is negative, the manifolds are not orientable, i.e., they are homeomorphic to a Möbius band. Using $u^0 = P(\theta, \sigma) = P(4.0, 0.7)$, we find that the defect of the conjugacy is

$$\|u_p^1 - u_i^1\|_2 \approx 1.92 \times 10^{-6}.$$

5.5 Unstable manifolds of Wright's equation

In the next applications we will focus on Wright's equation with either $\alpha = 2.2$ or $\alpha = 9.0$.

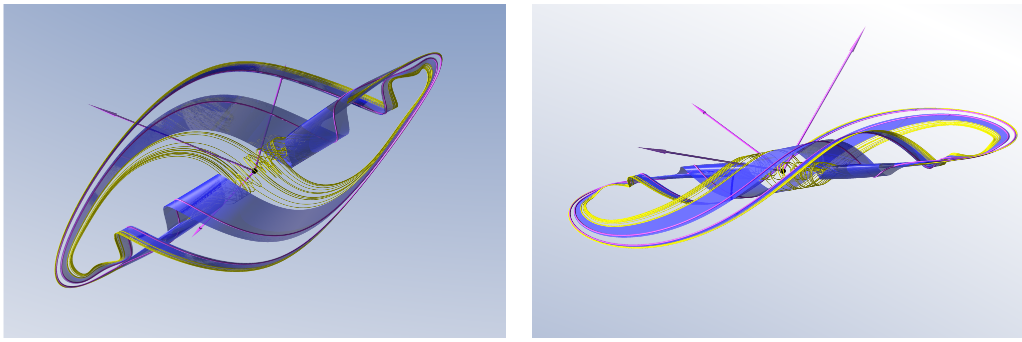

Figure 13: The attractor (yellow) and two-dimensional manifolds (blue) of the periodic orbits (magenta). The attractor is computed simply by integrating arbitrary initial conditions using a standard DDE integrator. The periodic orbit is computed using 140 Fourier modes. The unstable manifold is parameterized to Taylor order 51, where again each Taylor coefficient is computed with 140 Fourier modes.

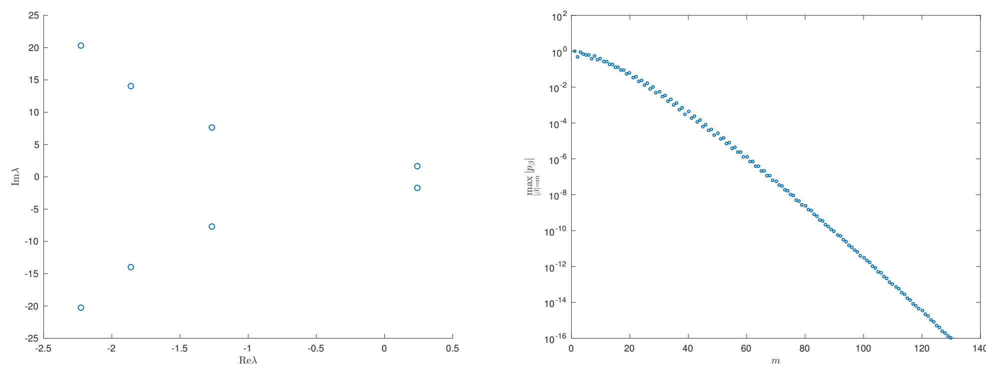

Figure 14: Left frame: the first 8 eigenvalues of the linearized Wright's equation at the point $u = 0$. Right frame: the decay of the coefficients of the parametrization of the unstable manifold at $u = 0$.

5.5.1 2D Unstable manifold of the equilibrium $u = 0$ for $\alpha = 2.2$.

For $\alpha = 2.2$ the linearized Wright's equation at the equilibrium $u = 0$ has exactly two unstable directions, with corresponding (complex conjugate) eigenvalues

$$\begin{aligned} \lambda_+ &= W_0(-2.2) &&\approx 0.24151{+}1.71102 \\ \lambda_- &= W_{-1}(-2.2) &&\approx 0.24151{-}1.71102. \end{aligned}$$

We parametrize the unstable manifold up to 130th order, using $131 \times 131 = 17161$ Taylor coefficients, shown in figure 14. The resulting manifold is illustrated in figure 15. We choose the eigenfunctions $\xi^0 e^{\lambda_\pm s}$, with $\xi^0 = 1.05$. Using $u^0 = P(0.3 + 0.4i, 0.3 - 0.4i)$, we find that the defect of the conjugacy is

$$\|u_p^1 - u_i^1\|_2 \approx 8.47 \times 10^{-7}.$$

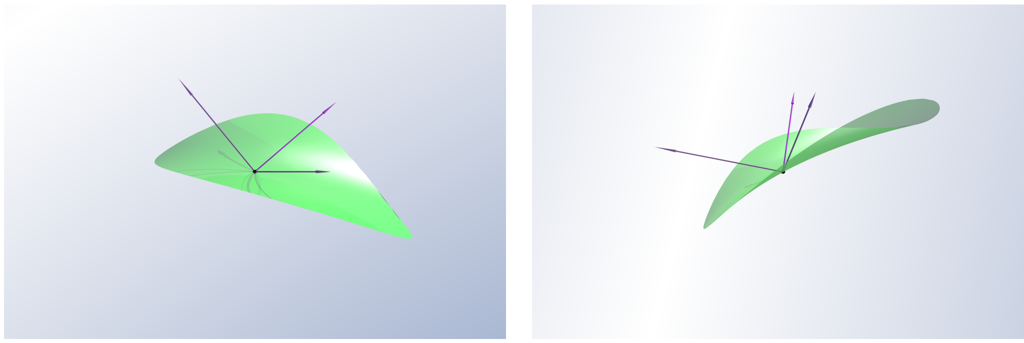

Figure 15: The two-dimensional manifold at $u = 0$ (green) as seen from two different angles.

5.5.2 4D Unstable manifold of the equilibrium $u = 0$ for $\alpha = 9.0$.

For $\alpha = 9.0$ the linearized Wright's equation at the equilibrium $u = 0$ has exactly four unstable directions, with two pairs of corresponding (complex conjugate) eigenvalues. We divide the eigenvalues into fast and slow subsystems, i.e.

$$\begin{aligned} \lambda_+^f &= W_0(-9) \approx 1.28926{+}2.11767i & \lambda_+^s &= W_1(-9) \approx 0.13390{+}7.87099i \\ \lambda_-^f &= W_{-1}(-9) \approx 1.28926{-}2.11767i & \lambda_-^s &= W_{-2}(-9) \approx 0.13390{-}7.87099i. \end{aligned}$$

We parametrize the unstable manifold up to 34th order, using $35^4 = 1500625$ Taylor coefficients. We choose a scaling of $\xi^0 = 1.0$ for the fast eigenfunctions and $\xi^0 = 0.15$ for the slow eigenfunctions. This parametrization also gives us a parametrization for a two dimensional fast and slow subsystem. These are simply given by

$$\mathcal{P}_{jk}^f = \mathcal{P}_{jk00} \qquad\qquad \mathcal{P}_{jk}^s = \mathcal{P}_{00jk}.$$

The decay of the coefficients, as well as those of the corresponding fast and slow subsystems are shown in figure 16. These particular fast and slow submanifolds of the unstable manifold are shown in figure 17.

We visualize the boundary of our total four dimensional manifold as a family of tori. If we take $c \in [0, 1]$ then we can define a torus T_c by setting

$$T_c := \{\mathcal{P}(z_1, \overline{z}_1, z_2, \overline{z}_2) : |z_1|^2 = c^2, |z_2|^2 = 1 - c^2\}.$$

Several of these tori have been plotted in figure 18. Using $u^0 = P(0.05 + 0.15i, 0.05 - 0.15i, 0.1 + 0.1i, 0.1 - 0.1i)$, we find that the defect of the conjugacy is

$$\|u_p^1 - u_i^1\|_2 \approx 2.70 \times 10^{-7}.$$

5.5.3 3D Unstable manifold of a periodic orbit.

After the bifuraction at $\alpha = 5\pi/2$ an unstable periodic orbit appears. At $\alpha = 9$, this unstable periodic orbit has a period of $T \approx 0.805$. This periodic orbit has two (complex conjugate) unstable Floquet multipliers whose values are approximately equal to $-0.19 \pm 2.72i$. After refining this, we then find that the corresponding complex Floquet exponents are given by

$$\lambda_+ \approx 1.24611 + 2.03632 \qquad\qquad \lambda_- \approx 1.24611 - 2.03632.$$

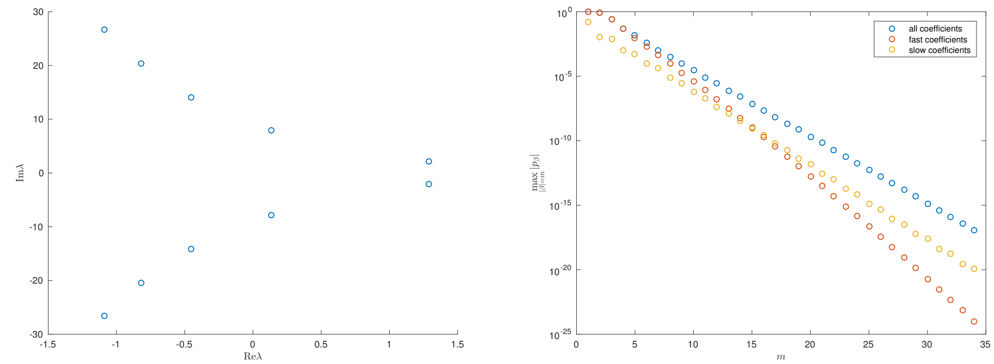

Figure 16: Left frame: the first 10 eigenvalues of the linearized Wright's equation at the point $u = 0$. Right frame: the decay of the coefficients of the parametrization of the unstable manifold at $u = 0$.

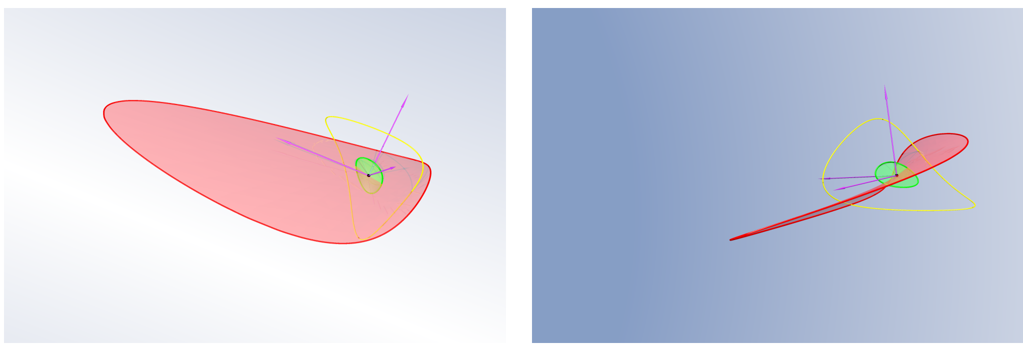

Figure 17: The two-dimensional fast manifold (red) and the two-dimensional slow manifold (green) manifold at $u = 0$ as seen from two different angles. The unstable periodic orbit of period $T \approx 0.805$ is shown in yellow. The manifolds seem to intersect one another (and the periodic orbit) because of the projection to 3 dimensions.

We parametrize the unstable manifold up to 42nd order and 22 Fourier modes, using $43\times 43\times(2\times 22+1) = 79380$ Fourier-Taylor coefficients. For the scaling we choose the eigenfunction ξ such that $\|\xi\|_2 = 2.5$, where we used the ℓ^2 norm on the space of Fourier-coefficients. The decay of these coefficients is shown in figure 19.

The local unstable manifold is a solid torus in $\mathcal{C}_\tau$. The boundary of this manifold actually extends quite "far" from the periodic orbit. This can readily be seen from the fact that while we can bound $\|v(\theta)\| \leq 1.2$ in $\mathcal{C}_\tau$, it is possible to find $|z| < 1$ and θ such that $\|\mathcal{P}(\theta, z, \overline{z})\| \geq 40$.

In order to obtain a clear picture, we picture the submanifold consisting of the image of all $z \in \mathbb{D}$ such that $|z| = 0.25$ in figure 20. For $|z| = 0.25$ we can calculate that $\|\mathcal{P}(\theta, z, \overline{z})\| \leq 5$. Equivalently, the submanifold in 20 would be the boundary (i.e., the points corresponding to $|z| = 1$) of the unstable manifold had we chosen a scaling of $\|\xi\|_2 = 0.25 \times 2.5 = 0.625$ instead. Using $u^0 = P(\theta, z, \overline{z}) = P(0.3, 0.15 + 0.1i, 0.15 - 0.1i)$, we find that the defect of the conjugacy is

$$\|u_p^1 - u_i^1\|_2 \approx 4.30 \times 10^{-6}.$$

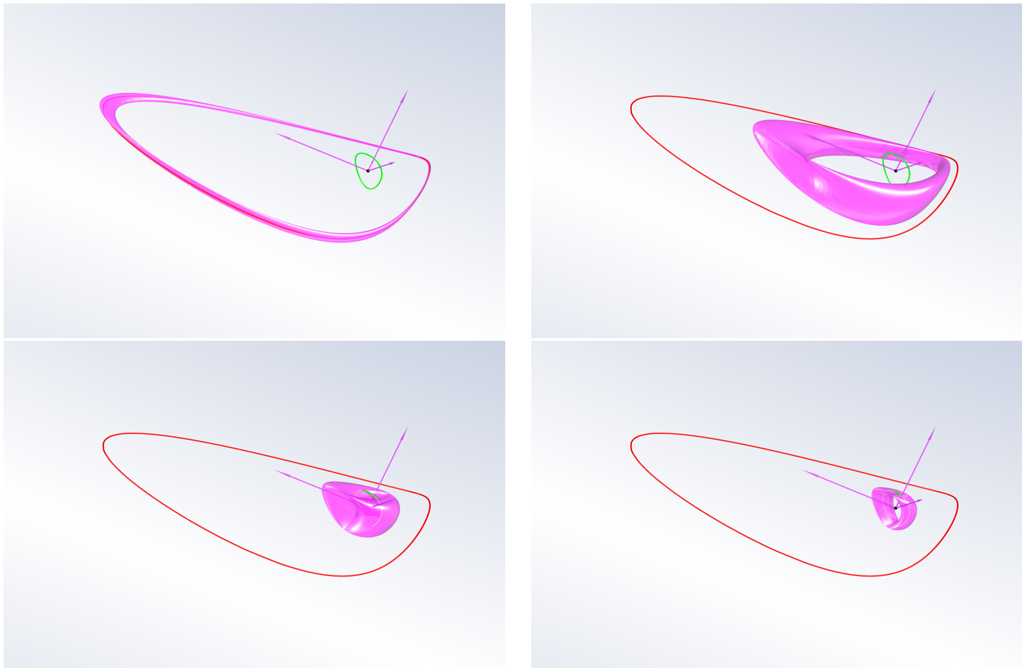

Figure 18: Several tori along the boundary of the 4D unstable manifold of the $u = 0$ equilibrium of Wright's equation for $\alpha = 9.0$. Depicted are the tori corresponding to $c \in \{0.99, 0.61, 0.21, 0.08\}$

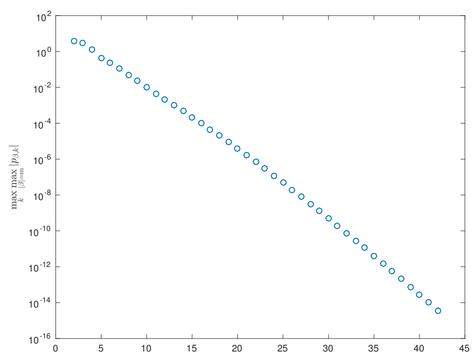

Figure 19: The decay of the coefficients computed for the parametrization of the unstable manifold, corresponding to the minimal periodic solutions of the cubic Ikeda equation.

5.6 Unstable manifold of a state dependent delay equation

For $\alpha = 2.2$ and all ϵ, the linearized equation at the equilibrium $u = 0$ has exactly two unstable directions, with corresponding (complex conjugate) eigenvalues

$$\lambda_+ = W_0(-2.2) \approx 0.24151 + 1.71102 \qquad \lambda_- = W_{-1}(-2.2) \approx 0.24151 - 1.71102.$$

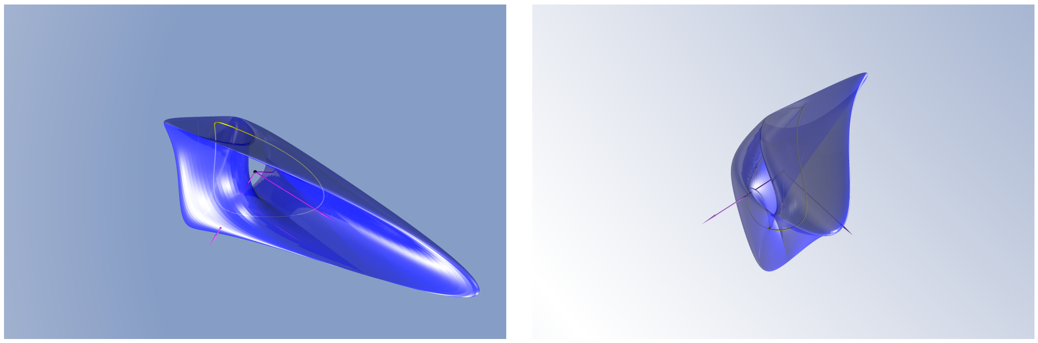

Figure 20: The periodic orbit (yellow) and two-dimensional submanifold (blue) of the unstable manifold of the periodic orbit corresponding to $|z| = 0.25$.

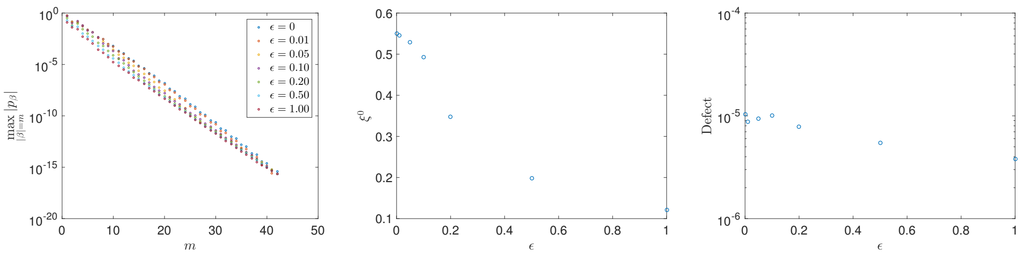

Figure 21: Left frame: The decay of the parametrizations. Middle frame: the scaling used for each ϵ. Right frame: the defect in the conjugacy for each value of ϵ.

We will, in the following, assume (and later check that) that the state dependent delay, given by $\tau(u(t)) = 1 - \epsilon u(t)$ satisfies $0 \le \tau \le 2$. We parametrize the unstable manifold up to 42nd order, using $43 \times 43 = 1849$ Taylor coefficients. The decay of the coefficients, for different values of ϵ, is illustrated in figure 21. For each value of ϵ, a slightly different scaling is optimal. These are shown in the same figure. Finally, although the maximal relevant delay might vary, depending on ϵ, we chose to evaluate the resulting parametrization using the delay embedding coordinates corresponding to $\{-1, -0.5, 0\}$. The resulting manifolds are shown in Figure 22.

Using $u^0 = P(0.3 + 0.2i, 0.3 - 0.2i)$, we have also plotted the defects in the last frame of figure 21.

6 Conclusions

In this paper we developed parameterization methods for unstable manifolds of both equilibrium and periodic solutions of delay differential equations (DDEs). After reviewing the classical reformulation of a DDE as an ordinary differential equation (ODE – on a function space) we studied first a flow conjugacy equation defining chart/covering maps for the local unstable manifolds, and then an infinitesimal version of the conjugacy. The infinitesimal version involves only the vector field/ODE derived from the delay equation (rather than the unknown flow), the eigendate associated with the equilibrium/periodic solution, and has only the desired parameterization as an unknown.

We then solved the infinitesimal conjugacy equation via formal series methods: Taylor

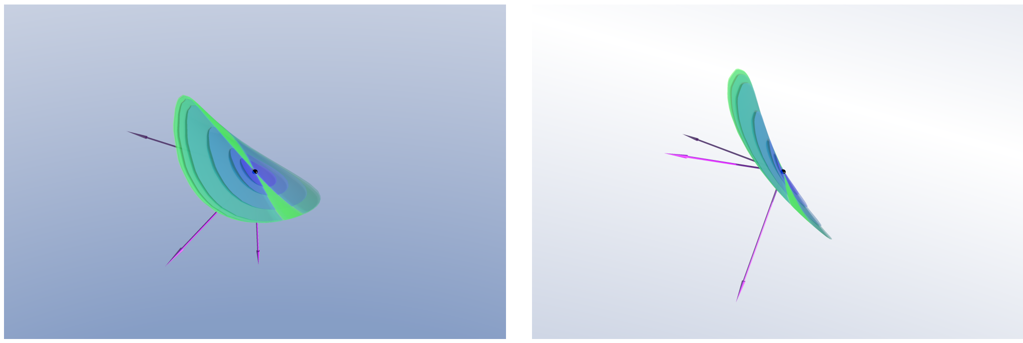

Figure 22: The unstable manifold of the state-dependent perturbation of Wright's equation, for several values of ϵ. The green manifold corresponds $\epsilon = 0$, while the dark blue one at the centre corresponds to $\epsilon = 1$. Note that while these manifolds do lie closely together, they do not exactly overlap.

methods were used in the equilibrium case and Fourier-Taylor methods in the periodic case. In both cases the series involve exponential weight functions which recover the backwards time trajectories of points on the manifold. The correct exponential weights fall out of our formal computations, once the DDE is properly reformulated as an ODE on a function space. This fact motivates the careful review of the ODE set-up early in the paper.

Next we gave a power matching argument which led to linear equations for the unknown series coefficients, i.e. the jets of the unstable manifold. We developed numerical algorithms for recursively solving these linear equations, leading to polynomial approximations of any desired order. The power matching scheme has a technical flavor and concrete examples are needed to illustrate its utility. We therefore applied our method to several dynamical situations in two different example problems: the cubic Ikeda equation and Wright's equation. We provide worked examples of the coefficient computation for equilibria having 1, 2, and 4 unstable directions and for periodic solutions having 1 and 2 unstable Floquet multipliers. The example computations demonstrate that our method does not apply just to one and two dimensional manifolds. In all cases we computed the expansions to high order to illustrate the automatic flavor of the computations, i.e. that once the correct homological equations are derived the order of the computation appears simply as a loop parameter. Many of our example computations involve systems with only a single constant delay, but we also provide an example of the use of our method for the case of an equation with a state dependent delay.

Both the example systems considered in the present work involved polynomial nonlinearities, and an interesting future project would be to implement our methods for systems with more general nonlinearities such as the Ikeda equation (trigonometric nonlinearity) or the Mackey-Glass equation (rational nonlinearity with non-integer powers). Numerical implementation for such systems could exploit techniques of automatic differentiation. See for example the work of [28, 51, 42] for a dynamical systems perspective on automatic differentiation close to the philosophy of the present work, or the classic text of [45] for a presentation closer to the tradition of computer science. It is also clear that our method applies to equations involving multiple delays, to systems with "continuous delays" (i.e. systems where the delay is given by an integral over the history of the solution), and even to systems of scalar delay equations. Working out the implementation details for some of these extensions would make another interesting future project. It should also be possible to extend the methods developed here to parabolic PDEs with delay terms, but we have not explored this possibility in any detail.

The computations in the present work result in polynomial approximations of the local unstable manifolds, and we have made no effort to extend our local manifolds via numerical integration. However, by combining our methods with continuation methods developed for delay equations in [24, 47, 63], one should be able to compute larger sections of the unstable manifolds than could be computed with either technique singly. This would make an excellent topic for a future study.

The focus of the present work is on semi-numerical methods for computing high order expansions of invariant manifolds for delay equations, and we have made only nominal efforts to quantify the errors in our computations. Yet there is a growing literature devoted to validated numerics for parameterized invariant manifolds for equilibria and periodic orbits. The works of [39, 61, 60, 12] would seem to suggest that mathematically rigorous, a-posteriori, computer assisted error bounds for our unstable manifold expansions are not too far out of reach. We are also strongly encouraged by the rigorous computer assisted Fourier analysis of periodic solutions of delay differential equations developed in [48, 44, 49, 43]. Indeed we have done some preliminary work on validating our results, and these results appear quite promising. A manuscript devoted to this topic is in preparation.

One exciting feature of this kind of constructive, a-posteriori, computer assisted analysis is that it may be possible to prove directly the existence of invariant objects for systems such as state dependent delay equations or equations with both positive and negative delays, where a-priori results are either unavailable or very difficult to obtain. Computer assisted proofs of chaos could be built on such methods by studying intersections of stable and unstable manifolds of periodic orbits, following the approach and references discussed in [57, 72, 10, 50, 15].

References

[1] Alfredo Bellen and Marino Zennaro. *Numerical methods for delay differential equations.* Numerical Mathematics and Scientific Computation. Oxford University Press, Oxford, 2013. First paperback reprint of the 2003 original [MR1997488].

[2] M. Breden, J.P. Lessard, and J.D. Mireles James. Computation of maximal local (un)stable manifold patches by the parameterization method. *Indagationes Mathematicae*, 27(1):340–367, 2016.

[3] Maxime Breden, Jean-Philippe Lessard, and Jason D. Mireles James. Computation of maximal local (un)stable manifold patches by the parameterization method. *Indag. Math. (N.S.)*, 27(1):340–367, 2016.

[4] X. Cabré, E. Fontich, and R. de la Llave. The parameterization method for invariant manifolds i: manifolds associated to non-resonant subspaces. *Indiana Univ. Math. J.*, 52:283–328, 2003.

[5] X. Cabré, E. Fontich, and R. de la Llave. The parametrization method for invariant manifolds ii: regularity with respect to parameters. *Indiana Univ. Math. J.*, 52:283–328, 2003.

[6] X. Cabré, E. Fontich, and R. de la Llave. The parametrization method for invariant manifolds iii: overview and applications. *Journal of Differential Equations*, 218(2):444–515, 2005.

[7] Renato C. Calleja, Alessandra Celletti, and Rafael de la Llave. A KAM theory for conformally symplectic systems: efficient algorithms and their validation. *J. Differential Equations*, 255(5):978–1049, 2013.

[8] Renato C. Calleja, Tony Humphries, and Bernd Krauskopf. Resonance phenomena in a scalar delay differential equation with two state-dependent delays. *(Submitted)* `https://arxiv.org/abs/1607.02683`, 2016.

[9] Sue Ann Campbell. Calculating center manifolds for delay differential equations using Maple$^{\text{TM}}$. In *Delay differential equations*, pages 221–244. Springer, New York, 2009.

[10] Maciej J. Capiński. Computer assisted existence proofs of Lyapunov orbits at L_2 and transversal intersections of invariant manifolds in the Jupiter-Sun PCR3BP. *SIAM J. Appl. Dyn. Syst.*, 11(4):1723–1753, 2012.

[11] R. Castelli, J.-P. Lessard, and J.D. Mireles-James. Parametrization of invariant manifolds for periodic orbits (i): efficient numerics via the floquet normal form. *SIAM Journal on Applied Dynamical Systems*, 14:132–167, 2015.

[12] Roberto Castelli, Jean-Philippe Lessard, and J. D. Mireles James. Parameterization of invariant manifolds for periodic orbits (ii): a-posteriori analysis and computer assisted error bounds. *(Submitted)*, 2016.

[13] G. M. Constantine and T. H. Savits. A multivariate Faà di Bruno formula with applications. *Trans. Amer. Math. Soc.*, 348(2):503–520, 1996.

[14] R. de la Llave, A. González, À. Jorba, and J. Villanueva. KAM theory without action-angle variables. *Nonlinearity*, 18(2):855–895, 2005.

[15] Rafael de la Llave and J. D. Mireles James. Connecting orbits for compact infinite dimensional maps: computer assisted proofs of existence. *SIAM Journal on Applied Dynamical Systems*, 15(n):1268–1323, 2016.

[16] Jayme De Luca, Nicola Guglielmi, Tony Humphries, and Antonio Politi. Electromagnetic two-body problem: recurrent dynamics in the presence of state-dependent delay. *J. Phys. A*, 43(20):205103, 20, 2010.

[17] Michael Dellnitz, Mirko Hessel-Von Molo, and Adrian Ziessler. On the computation of attractors for delay differential equations. *(submitted)*, 2015.

[18] K. Engelborghs, T. Luzyanina, and D. Roose. Numerical bifurcation analysis of delay differential equations using DDE-BIFTOOL. *ACM Trans. Math. Software*, 28(1):1–21, 2002.

[19] G. Farkas. Unstable manifolds for RFDEs under discretization: the Euler method. *Comput. Math. Appl.*, 42(8-9):1069–1081, 2001. Numerical methods and computational mechanics (Miskolc, 1998).

[20] Gyula Farkas. Discretizing hyperbolic periodic orbits of delay differential equations. *ZAMM Z. Angew. Math. Mech.*, 83(1):38–49, 2003.

[21] Jordi-Lluís Figueras, Marcio Gameiro, Jean-Philippe Lessard, and Rafael de la Llave. A framework for the numerical computation and a posteriori varification of invariant objects of evolution equations. *(Submitted)*, 2016.

[22] Harold Froehling, J. P. Crutchfield, Doyne Farmer, N. H. Packard, and Rob Shaw. On determining the dimension of chaotic flows. *Phys. D*, 3(3):605–617, 1981.

[23] Roy H. Goodman and Jacek K. Wróbel. High-order bisection method for computing invariant manifolds of two-dimensional maps. *Internat. J. Bifur. Chaos Appl. Sci. Engrg.*, 21(7):2017–2042, 2011.

[24] Kirk Green, Bernd Krauskopf, and Koen Engelborghs. One-dimensional unstable eigenfunction and manifold computations in delay differential equations. *J. Comput. Phys.*, 197(1):86–98, 2004.

[25] Antoni Guillamon and Gemma Huguet. A computational and geometric approach to phase resetting curves and surfaces. *SIAM J. Appl. Dyn. Syst.*, 8(3):1005–1042, 2009.

[26] Jack Hale. *Theory of functional differential equations.* Springer-Verlag, New York-Heidelberg, second edition, 1977. Applied Mathematical Sciences, Vol. 3.

[27] Jack K. Hale and Sjoerd M. Verduyn Lunel. *Introduction to functional-differential equations*, volume 99 of *Applied Mathematical Sciences.* Springer-Verlag, New York, 1993.

[28] A. Haro. Automatic differentiation methods in computational dynamical systems: Invariant manifolds and normal forms of vector fields at fixed points. IMA Note.

[29] A. Haro, M. Canadell, J-LL. Figueras, A. Luque, and J-M. Mondelo. *The parameterization method for invariant manifolds: from theory to effective computations*, volume -. Springer-Verlag, Berlin, 2016.

[30] À. Haro and R. de la Llave. A parameterization method for the computation of invariant tori and their whiskers in quasi-periodic maps: numerical algorithms. *Discrete Contin. Dyn. Syst. Ser. B*, 6(6):1261–1300 (electronic), 2006.

[31] A. Haro and R. de la Llave. A parameterization method for the computation of invariant tori and their whiskers in quasi-periodic maps: rigorous results. *J. Differential Equations*, 228(2):530–579, 2006.

[32] A. Haro and R. de la Llave. A parameterization method for the computation of invariant tori and their whiskers in quasi-periodic maps: explorations and mechanisms for the breakdown of hyperbolicity. *SIAM J. Appl. Dyn. Syst.*, 6(1):142–207 (electronic), 2007.

[33] Ferenc Hartung, Tibor Krisztin, Hans-Otto Walther, and Jianhong Wu. Functional differential equations with state-dependent delays: theory and applications. In *Handbook of differential equations: ordinary differential equations. Vol. III*, Handb. Differ. Equ., pages 435–545. Elsevier/North-Holland, Amsterdam, 2006.

[34] Xiaolong He and Rafael de la Llave. Construction of quasi-periodic solutions of state-dependent delay diferential equations by the parameterization method i: finitely differentiable, hyperbolic case. *(Submitted)*, 2015.

[35] Xiaolong He and Rafael de la Llave. Construction of quasi-periodic solutions of state-dependent delay differential equations by the parameterization method ii: Analytic case. *(submitted)*, 2015.

[36] T. Heil, I. Fischer, W. Elsäßer, B. Krauskopf, A. Gavrielides, and K. Green. Delay dynamics of semiconductor lasers with short external cavities: bifurcation scenarios and mechanisms. *Phys. Rev. E (3)*, 67(6):066214, 11, 2003.

[37] Gemma Huguet and Rafael de la Llave. Computation of limit cycles and their isochrons: fast algorithms and their convergence. *SIAM J. Appl. Dyn. Syst.*, 12(4):1763–1802, 2013.

[38] A. R. Humphries, O. A. DeMasi, F. M. G. Magpantay, and F. Upham. Dynamics of a delay differential equation with multiple state-dependent delays. *Discrete Contin. Dyn. Syst.*, 32(8):2701–2727, 2012.

[39] T. Johnson and W. Tucker. A note on the convergence of parametrised non-resonant invariant manifolds. *Qual. Theory Dyn. Syst.*, 10(1):107–121, 2011.

[40] G. Stephen Jones. The existence of periodic solutions of $f'(x) = -\alpha f(x-1)\{1+f(x)\}$. *J. Math. Anal. Appl.*, 5:435–450, 1962.

[41] G. Stephen Jones. On the nonlinear differential-difference equation $f'(x) = -\alpha f(x-1)\{1+f(x)\}$. *J. Math. Anal. Appl.*, 4:440–469, 1962.

[42] Àngel Jorba and Maorong Zou. A software package for the numerical integration of ODEs by means of high-order Taylor methods. *Experiment. Math.*, 14(1):99–117, 2005.

[43] Gábor Kiss and Jean-Philippe Lessard. Computational fixed-point theory for differential delay equations with multiple time lags. *J. Differential Equations*, 252(4):3093–3115, 2012.

[44] Gábor Kiss and Jean-Philippe Lessard. Tapidly and slowly oscillating periodic oscillations of a delayed van der pol oscillator. *(submitted)*, 2015.

[45] Donald E. Knuth. *The art of computer programming. Vol. 2.* Addison-Wesley, Reading, MA, 1998. Seminumerical algorithms, Third edition [of MR0286318].

[46] B. Krauskopf, H.M. Osinga, E.J. Doedel, M.E. Henderson, J.M. Guckenheimer, A. Vladimirsky, M. Dellnitz, and O. Junge. A survey of methods for computing (un)stable manifolds of vector fields. *Int.J. Birfurcation & Chaos*, 15(3):763–791, 2005.

[47] Bernd Krauskopf and Kirk Green. Computing unstable manifolds of periodic orbits in delay differential equations. *J. Comput. Phys.*, 186(1):230–249, 2003.

[48] Jean-Philippe Lessard. Recent advances about the uniqueness of the slowly oscillating periodic solutions of Wright's equation. *J. Differential Equations*, 248(5):992–1016, 2010.

[49] Jean-Philippe Lessard. Delay differential equations and continuation. *Lecture notes for the AMS short course on rigorous numerics in dynamics*, 2015.

[50] Jean-Philippe Lessard, Jason D. Mireles James, and Christian Reinhardt. Computer assisted proof of transverse saddle-to-saddle connecting orbits for first order vector fields. *J. Dynam. Differential Equations*, 26(2):267–313, 2014.

[51] J.P. Lessard, J. D. Mireles James, and J. Ransford. Automatic differentiation for fourier series and the radii polynomial approach. *(To appear in Physica D)*, 2016.

[52] Xuemei Li and R. de la Llave. Construction of quasi-periodic solutions of delay differential equations via kam techniques. *Journal of Differential Equaitons*, (247):822–865, 2009.

[53] J. Mireles-James and K. Mischaikow. Rigorous a-posteriori computation of (un)stable manifolds and connecting orbits for analytic maps. *SIAM Journal on Applied Dynamical Systems*, 12(2):957–1006, 2013.

[54] J. D. Mireles James. Computer assisted error bounds for linear approximation of (un)stable manifolds and rigorous validation of higher dimensional transverse connecting orbits. *Commun. Nonlinear Sci. Numer. Simul.*, 22(1-3):1102–1133, 2015.

[55] J. D. Mireles James. Fourier-taylor approximation of unstable manifolds for compact maps: Numerical implementation and computer assisted error bounds. *(To appear in Foundations of Computational Mathematics)*, 2016.

[56] J. D. Mireles James and Hector Lomelí. Computation of heteroclinic arcs with application to the volume preserving Hénon family. *SIAM J. Appl. Dyn. Syst.*, 9(3):919–953, 2010.

[57] Arnold Neumaier and Thomas Rage. Rigorous chaos verification in discrete dynamical systems. *Phys. D*, 67(4):327–346, 1993.

[58] Roger D. Nussbaum. Periodic solutions of analytic functional differential equations are analytic. *Michigan Math. J.*, 20:249–255, 1973.

[59] N. H. Packard, J. P. Crutchfield, Doyne Farmer, and Rob Shaw. Geometry from a time series. *Physical Review Letters*, 45(9):712–716, 1980.

[60] Christian Reinhardt and J.D. Mireles James. Fourier-taylor parameterization of unstable manifolds for parabolic partial differential equations: Formalism, implementation, and rigorous validation. *(submitted)*, 2016.

[61] Christian Reinhardt, J. B. Van den Berg, and J. D. Mireles James. Computing (un)stable manifolds with validated error bounds: non-resonant and resonant spectra. *Journal of Nonlinear Science*, 26:1055–1095, 2016.

[62] Dirk Roose, Tatyana Luzyanina, Koen Engelborghs, and Wim Michiels. Software for stability and bifurcation analysis of delay differential equations and applications to stabilization. In *Advances in time-delay systems*, volume 38 of *Lect. Notes Comput. Sci. Eng.*, pages 167–181. Springer, Berlin, 2004.

[63] Tuhin Sahai and Alexander Vladimirsky. Numerical methods for approximating invariant manifolds of delayed systems. *SIAM J. Appl. Dyn. Syst.*, 8(3):1116–1135, 2009.

[64] Giovanni Samaey, Koen Engelborghs, and Dirk Roose. Numerical computation of connecting orbits in delay differential equations. *Numer. Algorithms*, 30(3-4):335–352, 2002.

[65] Tim Sauer, James A. Yorke, and Martin Casdagli. Embedology. *J. Statist. Phys.*, 65(3-4):579–616, 1991.

[66] Jan Sieber and Bernd Krauskopf. Bifurcation analysis of an inverted pendulum with delayed feedback control near a triple-zero eigenvalue singularity. *Nonlinearity*, 17(1):85–103, 2004.

[67] J. C. Sprott. A simple chaotic delay differential equation. *Phys. Lett. A*, 366(4-5):397–402, 2007.

[68] Robert Szczelina and Piotr Zgliczyński. Algorithm for rigorous integration of delay differential equations and the computer-assisted proof of periodic orbits in the mackey-glass equation. *(Submitted)* http://ww2.ii.uj.edu.pl/~zgliczyn/papers/delay/main-dde.pdf, 2016.

[69] Floris Takens. Detecting strange attractors in turbulence. In *Dynamical systems and turbulence, Warwick 1980 (Coventry, 1979/1980)*, volume 898 of *Lecture Notes in Math.*, pages 366–381. Springer, Berlin-New York, 1981.

[70] J. B. van den Berg and J. D. Mireles James. Parametrization of slow-stable manifolds and their invariant vector bundles: theory and numerical implementaiton. *Discrete Contin. Dyn. Syst.*, 36(9), 2016.

[71] Hans-Otto Walther. Topics in delay differential equations. *Jahresber. Dtsch. Math.-Ver.*, 116(2):87–114, 2014.

[72] Daniel Wilczak and Piotr Zgliczyński. Heteroclinic connections between periodic orbits in planar restricted circular three body problem. II. *Comm. Math. Phys.*, 259(3):561–576, 2005.

[73] E. M. Wright. A non-linear difference-differential equation. *J. Reine Angew. Math.*, 194:66–87, 1955.

[74] Jacek K. Wróbel and Roy H. Goodman. High-order adaptive method for computing two-dimensional invariant manifolds of three-dimensional maps. *Commun. Nonlinear Sci. Numer. Simul.*, 18(7):1734–1745, 2013.